Efficient WLAN Link Simulations by Means of EESM

Author:
Emmanouil Logothetis

Thesis Commitee:
Prof. Georgios Karystinos (Supervisor)
Prof. Athanasios Liavas
Prof. Aggelos Bletsas

A thesis submitted in fulfillment
of the requirements for the degree of
Diploma in Electrical and Computer Engineering

Technical University of Crete
School of Electrical and Computer Engineering

Technical University of Greece
Chania, Greece

October 2021

Contents

Abstract

The widespread use of wireless local area networks (WLANs) in recent years and the continued need of higher transmission data rates resulted in the fast growth of WLAN systems. The simulation complexity of such systems however is huge. In this thesis, we focus on the IEEE 802.11n standard, which is based on high-throughput (HT) orthogonal frequency-division multiplexing (OFDM), and provide low time-complexity simulations by means of the exponential effective SNR mapping (EESM) method. The EESM method is a fundamental tool for evaluating and studying next generation OFDM-based wireless systems. It maps the set of different SNR values per subcarrier into a single effective flat-fading SNR, at which the system has the same performance. The EESM method is implemented for SISO, SIMO 1x2, and MIMO 2x2 configurations, in conjunction with the IEEE TGn Model-B frequency-selective channel. The simulator is based on the Matlab WLAN Toolbox. Full link simulations are performed to obtain the BER vs post-processing SNR curves for 20MHz channels, which are compared to the curves obtained through the EESM method. Extensive simulations indicate that the low-complexity EESM-based link simulations provide reliable BER vs post-processing SNR estimates. The latter makes EESM acceptable for abstraction in system level simulation to improve time efficiency.

Acknowledgments

The completion of this thesis marks the end of my studies towards the Diploma degree in Electrical and Compute Engineering. Also it marks the end of five years of a magic and challenging journey which gave me a lot of background theory and the knowledge to research and study all the fields that comprise the subject of ECE.

I would like to recognize the invaluable assistance of Prof. Georgios Karystinos and thank him for his supervision and support. Besides my advisor, I would like to thank the rest of my dissertation committee: Prof. Aggelos Bletsas and Prof. Athanasios Liavas. I am especially deeply grateful to Prof. Liavas for his courses which pushed me to deal with the Wireless Communications object.

Last, but not least, my warm and heartfelt thanks go to my family for their tremendous support and the opportunity they gave to me to pursue all of my goals. I also want to express my gratitude for my friends, who've been with me throughout this journey.

List of Abbreviations

ADC	Analog to Digital Converter
AGC	Automatic Gain Control
AMC	Adaptive Modulation and Coding
AWGN	Additive White Gaussian Noise
BCC	Binary Convolutional Code
BPSK	Binary Phase Shift Keying
CFO	Carrier Frequency Offset
CKK	Complementary Code Keying
CP	Cyclic Prefix
CPE	Common Phase Error
CS	Cyclic Shift
EESM	Exponential Effective SNR Mapping
FEC	Forward Error Correction
GI	Guard Interval
HT-LTF	High Throughput Long Training Field
HT-SIG	High Throughput Signal Field
HT-STF	High Throughput Short Training Field
ICI	Intercarrier Interference
ISI	Intersymbol Interference
L-LTF	Legacy Long Training Field
L-SIG	Legacy Signal Field
L-STF	Legacy Short Training Field

LDPC	Low-Density Parity-Check code
LLR	Log Likelihood Ratio
LQM	Link Quality Metrics
MCS	Modulation Coding Scheme
MIMO	Multiple Input - Multiple Output
MISO	Multiple Input - Single Output
MLD	Maximum Likelihood Detector
MMSE	Minimum Mean Square Error
MRC	Maximum Ratio Combining
OFDM	Orthogonal Frequency-Division Multiplexing
PHY	Physical Layer
PN	Phase Noise
PPDU	Physical layer Protocol Data Unit
QAM	Quadrature Amplitude Modulation
QPSK	Quadrature Phase Shift Keying
SFO	Sampling Frequency Offset
SIMO	Single Input - Multiple Output
SISO	Single Input - Single Output
SNR	Signal to Noise Ratio
STBC	Space-Time Block Coding
WLAN	Wireless Local Area Network
ZF	Zero Forcing

Chapter 1

Introduction

1.1 Motivation

Wireless Local Access Networks (WLANs) commonly in the form of Wi-Fi (802.11) systems had become very popular in the decade 2000 - 2009. WLAN provides mobility to the users so that they can roam around within the coverage range of WLAN, it decreases the connectivity complexity and cost, and it also gives the possibility to hold the connection in areas where cables cannot be run such as outdoor areas. These advantages of WLAN, and the huge growth of it to provide high speed internet access at numerous locations, resulted in the replacement of cable Local Access Networks by WLANs. Nowadays wireless broadband is becoming a fact, as society is based on functions that require the use of the internet wherever. The users want to be able to stream HD videos and music, transfer large amounts of data, or make video conferences. With the onset of the COVID-19 pandemic, the usefulness of WLANs increased. As work and school shifted remotely, some networks saw an increase of 300% in video conferencing services (BITAG). Furthermore the global Wi-Fi traffic increased by 80% at the beginning of the pandemic as the Wi-Fi Alliance notes. The continued growth of the WLAN technology results in high complexity communication systems. Various MIMO schemes, modulation coding rates, and channel bandwidths are provided to increase the system throughput. Consequently, the evaluation of the performance of a system by means of classical link level simulations has high time complexity, which prevents the simulation of a system for each parameter it must be studied.

The purpose of the present thesis is to provide efficient time WLAN simulations by means of the Exponential Effective SNR Mapping (EESM) method. The EESM method has been proposed to decrease the simulation complexity for systems which use the OFDM technique. Since the modern WLAN systems use the OFDM technique, we study the EESM method in the standard 802.11n, one of the most fundamental of WLAN standards, as all the newly released amendments, e.g. 802.11ac, 802.11ax, are based on this principles. The time complexity of EESM is concentrated in the tuning procedure of the method. Once the

parameters of the method are specified, the system can be simulated with negligible time complexity.

1.2 Thesis Outline

The rest of the report is organized as follows. Chapter 2 contains a revision about IEEE 802.11 standards, the Orthogonal Frequency - Division Multiplexing technique, and the MIMO systems. In Chapter 3, the IEEE 802.11n PHY frames are demonstrated, followed by an explanation of the transmitter and the receiver operations in step-by-step details. In Chapter 4, HT MIMO OFDM systems are analyzed. Also the post-processing SNR is defined and relations between SNRs at different stages of the system are derived. Chapter 5 demonstrates the Exponential Effective SNR Mapping (EESM) method, the derivation of the EESM formula, and the calibration method of EESM parameters. In Chapter 6, the simulation environment and the numerical results are presented. Finally, Chapter 7 draws some concluding remarks and a summary of our findings.

Chapter 2

IEEE 802.11 Standards & Background Theory

2.1 IEEE 802.11 Standards

The first version of the 802.11 standard was ratified in 1997 by the IEEE 802 LAN/MAN standards committee after seven long years of development. Since 1997 many standards and amendments have been released which are deployed worldwide in unlicensed regions of the radio frequency spectrum. Over time, the maximum achievable transmission data rate has grown from 1 megabit per second (Mbps) to nearly 9.6 gigabit per second (Gbps). In Table 2.1 the released standards with they properties are presented.

By 1999, two amendments were made to the first standard proposed in 1997. The IEEE 802.11b is an extension to the previously-defined PHY with DSSS and used complementary-code keying (CCK) modulation scheme. It supports a data rate of 11Mbps. IEEE 802.11a specified a new radio-based PHY at that operates in different frequency band i.e. 5.2 GHz and used Orthogonal Frequency-Division Multiplexing (OFDM) transmission which allows data rates up to 54 Mbps. Although 802.11b may appear to be the older standard but the amendment for 802.11a was proposed before 802.11b [1]. Then in the year 2002 a new amendment to 802.11 was made i.e. 802.11g. This standard also used OFDM as being used in IEEE 802.11a and supported data rates up to 54 Mbps, but it used 2.4 GHz as a carrier, as it was used in 802.11b. The standard 802.11g provides good performance, but throughput given by this standard is not good enough to applications like video streaming and establishing multiple video conferencing sessions. That leads to the next amendment to this standard to support higher throughput. In 2007 a new amendment 802.11n specifications were released. The initial goal of this standard was to allow data rates of at least 100 Mbps. To increase throughput, multiple transmit and receive antennas (or MIMO) are being used and the access point is allowed to use 40 MHz channel and more sophisticated processing techniques. 802.11ac is the next amendment to the

IEEE 802.11 specification for Wireless Local Area Networks (WLANs). For 802.11ac, wider channels and up to eight input/output streams offer higher maximum throughputs. This increased throughput capability enables users to stream video to mobile devices at home or public mobile hot spots. The 802.11ax amendment introduces orthogonal frequency-division multiple access (OFDMA) to improve the overall spectral efficiency and higher-order 1024-point quadrature amplitude modulation (1024-QAM) support for increased throughput.

Table 2.1: WLAN 802.11 standards features.

Standard	**Release Year**	**Modulation**	**Base Frequency (GHz)**	**Bandwidth (MHz)**	**Maximum Throughput (Mbps)**	**Antenna Scheme**	**PPDU Format**
802.11	1997	DSSS	2.4	11	2	SISO	Non-HT
802.11b	1999	HR/ DSSS/CKK	2.4	11	11	SISO	Non-HT
802.11a	1999	OFDM	5	5,10,20	54	SISO	Non-HT
802.11g	2003	HR/ DSSS/CKK OFDM	2.4	5,10,11,20	54	SISO	Non-HT
802.11j	2004	OFDM	4.9 and 5	10,20	27	SISO	Non-HT
802.11n (Wi-Fi 4)	2009	OFDM	2.4 , 5	20, 40	< 600	MIMO, up to four streams	HT
802.11p	2010	OFDM	5	5, 10	27	SISO	Non-HT
802.11ad	2012	SC/OFDM	60	1760 , 2640	< 7000	MIMO, single stream with beamforming	DMG
802.11ac (Wi-Fi 5)	2013	OFDM	5	20, 40, 80, 160, 80+80	< 7000	DL MU-MIMO, up to eight streams	VHT
802.11ah	2016	OFDM	<1	1,2,4,8,16	346	DL MU-MIMO, up to four streams	S1G
802.11ax (Wi-Fi 6)	2021	OFDMA	2.4 and 5	20, 40, 80, 160, 80+80	< 9600	UL and DL MU-MIMO, up to eight streams	HE

2.2 Orthogonal Frequency Division Multiplexing (OFDM)

Orthogonal Frequency-Division Multiplexing is a method of digital modulation in which the available channel bandwidth is split into adjacent narrowband channels (called subcarriers or tones) and the high-data-rate stream is split into several low-data-rate streams which are multiplexed to the subcarriers and transmitted simultaneously. In addition, the subcarriers in an OFDM system are precisely orthogonal to one another. As a result, while the subcarriers are overlapping to maximize spectral efficiency, they do not cause adjacent channel interference. OFDM is well suited to wideband systems in frequency selective fading environments because it converts a wideband channel into a set of N_{FFT}

narrowband channels. Therefore, it does not required equalization, which has significant computational cost, but symbol-to-symbol decision for each information symbol. Only a few subcarriers are impacted by a deep fade or narrow band interference, which can be protected by forward error correction code. Each subcarrier is independently modulated by using any constellation scheme, such as Binary Phase-Shift Keying (BPSK), Quadrature Phase-Shift Keying (QPSK) and Quadrature Amplitude Modulation (QAM).

2.2.1 OFDM Guard Interval & Cyclic Extension

Intersymbol Interference

Due to the multipath phenomena, the received signal at the receiver is the sum of delayed replicas of the same transmitted signal. When the maximum delay is comparable with the symbol duration, intersymbol interference (ISI) is caused. This means that subsequent symbols interferes. A guard interval (GI) is inserted between OFDM base-band signal blocks to prevent intersymbol interference. To eliminate the ISI the guard interval duration must be chosen larger than the expected multipath delay spread in order that the delayed components of each symbol do not interfere with the next one. There are several options for GI. One choice of GI is zero padding. In this scheme, no waveform is transmitted in the GI duration. However, the zero-padded waveform prevents the intersymbol interference but intercarrier interference (ICI) can be caused. The cyclic prefix (CP) which proposed first time in [2] is a good substitute of the zero-padding GI as described below.

Intercarrier Interference

Intercarrier Interference (ICI) is an impairment well known to degrade performance of OFDM transmissions. Intercarrier interference is caused when subcarriers lose orthogonality. It arises from carrier frequency offsets (CFOs), from the Doppler spread due to channel time-variation and, to a lesser extent, from sampling frequency offsets (SFOs). To overcome the ICI problem, the OFDM symbol is cyclically extended along the guard time, so that any subcarrier coming from direct or delayed replicas of the signal will continue to have an integer number of cycles within an FFT interval of duration T [3]. This effectively simulates a channel performing cyclic convolution, which implies orthogonality over the channels when the CP is longer than the impulse response of the channel. The benefit of a cyclic prefix is twofold: it avoids both ISI (since it acts as a guard space) and ICI (since it maintains the orthogonality of the subcarriers). The basic disadvantage of the CP is that the transmitted energy increases with the length of the cyclic prefix.

2.2.2 OFDM Signal Generation

One OFDM symbol with duration T, has the following passband expression in the time domain

$$s(t) = \frac{1}{\sqrt{N_{\text{FFT}}}} \sum_{k=0}^{N_{\text{FFT}}-1} d_k e^{j2\pi f_k t} W_T(t) \tag{2.1}$$

where $f_k = {}^{k}/_{T}$ is the k-th frequency, d_k is the symbol modulating the k-th carrier during the whole OFDM symbol interval and $W_T(t)$ is the windowing function

$$W_T(t) = \begin{cases} 1 & t \in [0, T] \\ 0 & \text{otherwise} \end{cases} \tag{2.2}$$

Note that we would typically subtract ${}^{(N_{\text{FFT}}-1)}/_{2T}$ from all the frequencies above to center the baseband frequency content around the origin, but this is not shown, in order to keep the notation simple. Letting the OFDM symbol extend far beyond the period T, so as to produce a periodic signal $\tilde{s}(t)$, which in frequency domain can be expressed in the form

$$\tilde{S}(f) = \sum_{k=0}^{N_{\text{FFT}}-1} d_k \delta\Big(f - \frac{k}{T}\Big) \tag{2.3}$$

In general will consider that in one extended OFDM symbol, the subcarriers are windowed (multiplied) in continues time with a unitary amplitude rectangular pulse W_{T_p} of duration T_p as defined in Equation (2.2). The frequency spectrum for this continues rectangular pulse is given by its Fourier Transform

$$W_{T_p}(f) = T_p \frac{\sin(\pi T_p f)}{\pi T_p f} e^{-jT_p \pi f} = T_p \text{sinc}(T_p f) e^{-jT_p \pi f} \tag{2.4}$$

From the Convolution Theorem the spectrum $S(f)$ of a single OFDM symbol for a given interval it can be expressed as the frequency-domain convolution between the window $W_{T_p}(f)$ and the extended signal spectrum $\tilde{S}(f)$.

$$S(f) = W_{T_p}(f) * \sum_{k=0}^{N_{\text{FFT}}-1} d_k \delta\Big(f - \frac{k}{T}\Big) = \sum_{k=0}^{N_{\text{FFT}}-1} d_k W_{T_p}\Big(f - \frac{k}{T}\Big) \tag{2.5}$$

We can conclude that only for windows of duration $T_p = \{T, 2T, 3T, \dots\}$, which is called period extension (PE) of the symbol, the orthogonality of subcarriers still remain. As it discussed above, to prevent the ISI and ICI the OFDM symbol in practice is cyclic extended. Thus the N_{FFT} components are no longer orthogonal, although they remain centered at the same frequencies f_k. Therefore, in the reception branch, the samples of the cyclic extension must be discarded to re-create the original OFDM symbol thus obtaining a periodic signal block for the FFT to process.

Orthogonality of Subcarriers

The orthogonality of different subcarriers holds over an interval of length T if they are spaced apart by an integer multiple of $1/T$.

$$\int_0^T e^{-j2\pi f_n t} e^{j2\pi f_m t} \mathrm{d}t = \frac{e^{j2\pi(f_n - f_m)T} - 1}{j2\pi(f_n - f_m)} = \begin{cases} 1 & (f_n - f_m)T = 0 \\ 0 & (f_n - f_m)T \in \mathbb{Z}^* \end{cases} \tag{2.6}$$

Assuming ideal channel, due to the orthogonality of subcarriers the received signal $s(t)$ can be demodulated as follows:

$$\begin{aligned} & \int_0^T \sum_{n=0}^{N_{\mathrm{FFT}}-1} s(t) e^{-j2\pi f_m t} \mathrm{d}t \\ = & \int_0^T \sum_{n=0}^{N_{\mathrm{FFT}}-1} \frac{1}{N_{\mathrm{FFT}}} d_n e^{j2\pi f_n t} e^{-j2\pi f_m t} \mathrm{d}t \\ = & \sum_{n=0}^{N_{\mathrm{FFT}}-1} \frac{1}{N_{\mathrm{FFT}}} d_n \int_0^T e^{j2\pi f_n t} e^{-j2\pi f_m t} \mathrm{d}t \\ = & \, d_m \end{aligned} \tag{2.7}$$

The orthogonality of subcarriers it can be observed at the frequency domain of the signals as the main lobe of a signal occur when the nulls of other signals hold.

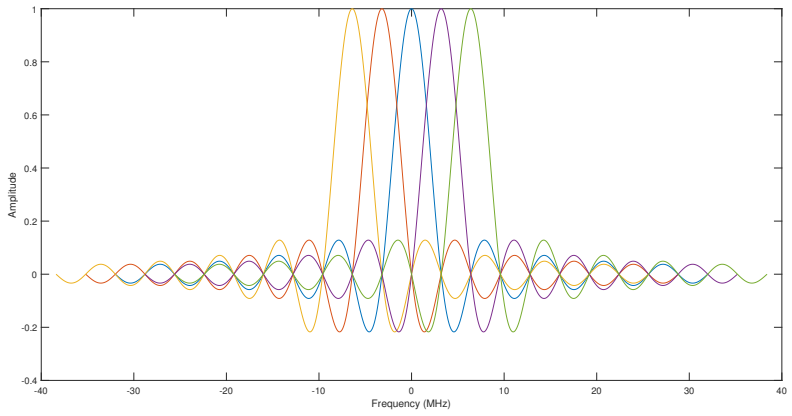

Figure 2.1: Orthogonal subcarriers in OFDM using window function with duration $T_p = T$.

2.2.3 OFDM in IEEE 802.11n

The IEEE 802.11n standard supports an OFDM system with bandwidth values 20 and 40 MHz. The Fourier transform symbol period, T, is 3.2μs in duration and the bandwidth of

each subcarrier $\Delta_F = 312.5$KHz. It uses a number of subcarriers which is a power of two for efficient FFT operations. The subcarriers are used for carrying data symbols and pilot signals. The number of data and pilot subcarriers are represented in Table 2.2. The pilot subcarriers are used to estimate and correct phase and frequency shifts over all OFDM symbols. The indices of pilot subcarriers are set scattered on the frequencies in order to be able to give an estimate of the whole bandwidth. The subcarriers that correspond at the DC and the higher and lower edges of the bandwidth are nulled to prevent interference from adjacent channels.

Table 2.2: Number of OFDM Subcarrier in 802.11n Standard.

Bandwidth (MHz)	**20**	**40**
FFT Size (N_{FFT})	64	128
Number Of Data SCs (N_{SD})	52	108
Number Of pilot SCs (N_{SP})	4	6
Total number of SCs (N_{ST})	56	114

To avoid ISI and ICI a guard interval is inserted with a cyclic prefix. The standard supports three different guard interval durations : normal guard interval $T_{\mathrm{GI}} = 800ns$, short GI $T_{\mathrm{GIS}} = 400ns$, and double guard interval $T_{\mathrm{GI2}} = 1600ns$. In the IEEE 802.11 standards, the symbols duration is $3.2\mu s$, and with the insertion of the normal guard interval duration $T_{\mathrm{GI}} = 800ns$ the receiver can handle a channel delay spread of $600ns$.

Figure 2.2: Cyclically extension of OFDM symbols in IEEE 802.11n.

The windowing function which is used in 802.11n is given by the expression

$$W_T(t) = \begin{cases} \sin^2\left(\frac{\pi}{2}\left(0.5 + \frac{t}{T_{\mathrm{TR}}}\right)\right) & -T_{\mathrm{TR}}/2 < t <, T_{\mathrm{TR}}/2 \\ 1 & T_{\mathrm{TR}}/2 \leq t < T - T_{\mathrm{TR}}/2 \\ \sin^2\left(\frac{\pi}{2}\left(0.5 - \frac{t-T}{T_{\mathrm{TR}}}\right)\right) & T - T_{\mathrm{TR}}/2 \leq t \leq T + T_{\mathrm{TR}}/2 \end{cases} \tag{2.8}$$

where T_{TR} is the window transition time.The extended waveform is windowed by pointwise multiplication in the time domain. The domain of the windowing function purposed to the reduction the out-of-band emissions which caused from the discontinuities produced from IFFT processing. After windowing is applied to each symbol, the trailling shoulder samples

are added to the leading shoulder samples of the next symbol, so in this manner reduces out-of-band emissions.

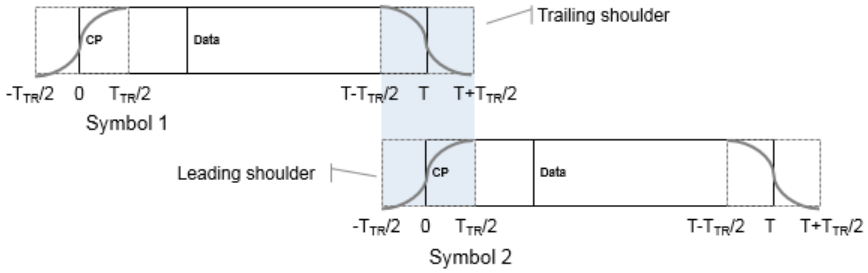

Figure 2.3: The effect of windowing process in two adjacent symbols.

2.3 Multiple Input - Multiple Output (MIMO)

A Multiple Input - Multiple Output system uses a multiple antennas at both the transmitter and receiver to succeed spatial diversity or to increase the data rate of wireless communication system. Spatial diversity provides higher Signal to Noise Ratio (SNR) without increasing the power of the transmitted signal. Using MIMO systems also provides the capability to increase the data rate without expanding the bandwidth of transmitted signal. This method is called spatial multiplexing.

Let N_{TX} be the number of transmit antennas and N_{RX} be the number of receive antennas, MIMO systems can be divided into three special categories :

- when $N_{\mathrm{TX}} = N_{\mathrm{RX}} = 1$ the system is called Single input - Single Output (SISO) system.
- when $N_{\mathrm{TX}} > 1, N_{\mathrm{RX}} = 1$ the system is called Multiple Input - Single Output (MISO) system.
- when $N_{\mathrm{TX}} = 1, N_{\mathrm{RX}} > 1$ the system is called Single Input - Multiple Output (SIMO) system.

2.3.1 Spatial Diversity

Spatial diversity is achieved by using SIMO, MISO or MIMO wireless communication systems where the transmission and the reception of the signal being over multiple independent channels.

Reception Diversity

Using N_{RX} antennas at the receiver the signal it can be transmitted over N_{RX} independent channels. The mathematical expression for the k-th symbol at the receiver is

$$\mathbf{y}_k = \mathbf{h}_k x_k + \mathbf{n}_k \tag{2.9}$$

where $\mathbf{y}_k$ is the vector with the N_{RX} symbols which have been received, $\mathbf{h}_k$ the channel response of the N_{RX} independent channels, x_k is the k-th transmitted symbol and $\mathbf{n}_k \sim \mathcal{CN}(\mathbf{0}, N_0\mathbf{I})$ the additive Guassian noise components. Maximum Ratio Combining method is the optimal decision for x_k as described at the following equation

$$r_k = \frac{\mathbf{h}_k^H}{||\mathbf{h}_k||_2^2}\mathbf{y}_k = x_k + \mathbf{z}, \quad \mathbf{z} \sim \mathcal{CN}\Big(\mathbf{0}, \frac{N_0}{||\mathbf{h}_k||_2}\Big) \tag{2.10}$$

Transmit Beamforming

The MRC technique is based on knowing the channel vector $\mathbf{h}_k$ at the receiver. Another linear technique to succeed diversity in a MISO system is transmit beamforming. Channel vector must be known at the transmitter and the transmitted symbols must been beamformed as follows

$$\mathbf{x}_k = \frac{\mathbf{h}_k^*}{||\mathbf{h}_k||_2} x_k \tag{2.11}$$

The received signal is the effect of superposition of all received components from different channels and given by the expression

$$y = \frac{1}{||\mathbf{h}_k||_2}(h_{1,k}h_{1,k}^* + \cdots + h_{N_{\mathrm{TX}},k}^* h_{N_{\mathrm{TX}},k})x_k + n_k = ||\mathbf{h}_k||_2 x_k + n_k \tag{2.12}$$

In the general case where there used multiple antennas at the transmitter and the receiver, transmit beamforming method can be applied by using the singular value decomposition (SVD) of the channel matrix $\mathbf{H}$. Channel matrix $\mathbf{H}$ with rank r may be expressed as

$$\mathbf{H} = \mathbf{U}\mathbf{\Sigma}\mathbf{V}^H \tag{2.13}$$

where $\mathbf{U}$ is an $N_{\mathrm{RX}} \times r$ matrix, $\mathbf{V}$ is an $N_{\mathrm{TX}} \times r$ matrix, and $\mathbf{\Sigma}$ is an $r \times r$ diagonal matrix with diagonal elements the singular values of the channel. The column vectors of the matrices $\mathbf{U}$ and $\mathbf{V}$ are orthonormal. Hence $\mathbf{U}^H\mathbf{U} = \mathbf{I}_r, \mathbf{V}^H\mathbf{V} = \mathbf{I}_r$. Processing the transmitted signal vector $\mathbf{x}$ of length r at the transmitter by the linear transformation

$$\mathbf{x}_v = \mathbf{V}\mathbf{\Sigma}^{-1}\mathbf{x} \tag{2.14}$$

then the received signal vector $\mathbf{y}$ is

$$\mathbf{y} = \mathbf{H}\mathbf{V}\mathbf{\Sigma}^{-1}\mathbf{x} + \mathbf{n}, \quad \mathbf{n} \sim \mathcal{CN}(\mathbf{0}_{N_{\mathrm{RX}}}, N_0\mathbf{I}_{N_{\mathrm{RX}}}) \tag{2.15}$$

After multiplied the received signal with the matrix $\mathbf{U}^H$ we have

$$\begin{aligned}\mathbf{r} &= \mathbf{U}^H\mathbf{y} = \mathbf{U}^H\mathbf{H}\mathbf{V}\mathbf{\Sigma}^{-1}\mathbf{x} + \mathbf{U}^H\mathbf{n} \\ &= \mathbf{U}^H\mathbf{U}\mathbf{\Sigma}\mathbf{V}^H\mathbf{V}\mathbf{\Sigma}^{-1}\mathbf{x} + \mathbf{U}^H\mathbf{n} = \mathbf{x} + \mathbf{U}^H\mathbf{n}\end{aligned} \tag{2.16}$$

Therefore, the elements of the received signal are decouptled and may be detected individually.

2.3.2 Space-Time Block Coding (STBC)

Space-Time Block Coding is a technique where the N_{SS} spatial streams are mapped into to N_{STS} space-time streams, which are mapped to N_{TX} transmit chains. Using the STBC method multiple copies of data streams transmitted over different antennas, and then the various received versions of the data is used to improve the reliability of data transfer. STBC technique is applicable only when the number of space time streams N_{STS} is greater than the number of spatial streams N_{SS}. Alamouti's scheme for $N_{\text{TX}} = 2$ and $N_{\text{RX}} = 1$ it is the only scheme that provides full transmit diversity gain with low complexity for a system with two antennas. The generator matrix for the Alamouti code is given as

$$\mathbf{G} = \begin{bmatrix} x_1 & x_2 \\ -x_2^* & x_1^* \end{bmatrix} \tag{2.17}$$

where x_1, x_2 are the two signal points being transmitted. The rows of the generator matrix corresponds to the symbols and the columns at the time slot that are being transmitted. Assuming that the channel is constant over the two time slots, at the receiver we can construct the vector

$$\begin{bmatrix} y_1 \\ y_2^* \end{bmatrix} = \begin{bmatrix} h_1 & h_2 \\ h_2^* & -h_1^* \end{bmatrix} \begin{bmatrix} x_1 \\ x_2 \end{bmatrix} + \begin{bmatrix} w_1 \\ w_2^* \end{bmatrix} \tag{2.18}$$

Defining the unitary matrix

$$\mathcal{H} = \frac{1}{||\mathbf{h}||_2} \begin{bmatrix} h_1 & h_2 \\ h_2^* & -h_1* \end{bmatrix} \tag{2.19}$$

and multiplied by left the vector $\mathbf{y}$ with the $\mathcal{H}^H$ the two decision statistics are

$$\begin{aligned}\begin{bmatrix} r_1 \\ r_2 \end{bmatrix} &= \mathcal{H}^H \begin{bmatrix} h_1 & h_2 \\ h_2^* & -h_1^* \end{bmatrix} \begin{bmatrix} x_1 \\ x_2 \end{bmatrix} + \mathcal{H}^H \begin{bmatrix} n_1 \\ n_2^* \end{bmatrix} \\ &= \begin{bmatrix} ||\mathbf{h}||_2 x_1 \\ ||\mathbf{h}||_2 x_2 \end{bmatrix} + \begin{bmatrix} \hat{n_1} \\ \hat{n_2} \end{bmatrix}.\end{aligned} \tag{2.20}$$

Therefore we can decide individual for the two symbols x_1, x_2 based on the values r_1, r_2. If the h_1, h_2 are independent the Alamouti scheme achieves diversity order 2. Alamouti scheme can be extended to multiple antennas on receiver with two antennas at the transmitter and

achieving the maximum possible diversity $N_{\mathrm{TX}}N_{\mathrm{RX}} = 2N_{RX}$ [4]. For Alamouti STBC modes in the general case, we define the $N_{\mathrm{RX}} \times 2$ channel matrix as

$$\mathbf{H} = \begin{bmatrix} \mathbf{h}_1 & \mathbf{h}_2 \end{bmatrix} = \begin{bmatrix} h_{11} & h_{12} \\ h_{21} & h_{22} \\ \vdots & \vdots \\ h_{N_{\mathrm{RX}}1} & h_{N_{\mathrm{RX}}2} \end{bmatrix} \tag{2.21}$$

Thus, $h_{m,n}$ is the channel coefficient from Tx antenna n to Rx antenna m. In addition, we define the vector

$$\mathbf{h} = \begin{bmatrix} \mathbf{h}_1 \\ \mathbf{h}_2 \end{bmatrix}. \tag{2.22}$$

On the receiver side combining two sequentially time slots we have

$$\begin{bmatrix} \mathbf{y}_1 \\ (\mathbf{y}_2)^* \end{bmatrix} = \begin{bmatrix} \mathbf{h}_1 & \mathbf{h}_2 \\ \mathbf{h}_2^* & -\mathbf{h}_1^* \end{bmatrix} \begin{bmatrix} x_1 \\ x_2 \end{bmatrix} + \begin{bmatrix} \mathbf{n}_1 \\ \mathbf{n}_2^* \end{bmatrix} \tag{2.23}$$

Defining the matrix $\mathcal{H}$ with dimensions $2N_{\mathrm{RX}} \times 2$ as follows

$$\mathcal{H} = \frac{1}{||\mathbf{h}||_2^2} \begin{bmatrix} \mathbf{h}_1 & \mathbf{h}_2 \\ \mathbf{h}_2^* & -\mathbf{h}_1^* \end{bmatrix} \tag{2.24}$$

and multiplying the Equation (2.23) by the hermitian transpose of the matrix $\mathcal{H}$ the estimates are transformed to

$$\begin{bmatrix} \hat{x}_1 \\ \hat{x}_2 \end{bmatrix} = \frac{1}{||\mathbf{h}||_2^2} \begin{bmatrix} \mathbf{h}_1^H & \mathbf{h}_2^T \\ \mathbf{h}_2^H & -\mathbf{h}_1^T \end{bmatrix} \begin{bmatrix} \mathbf{h}_1 & \mathbf{h}_{k,2} \\ \mathbf{h}_2^* & -\mathbf{h}_1^* \end{bmatrix} \begin{bmatrix} x_1 \\ x_2 \end{bmatrix} + \frac{1}{||\mathbf{h}||_2^2} \begin{bmatrix} \mathbf{h}_1^H & \mathbf{h}_2^T \\ \mathbf{h}_2^H & -\mathbf{h}_1^T \end{bmatrix} \begin{bmatrix} \mathbf{n}_1 \\ \mathbf{n}_2^* \end{bmatrix}. \tag{2.25}$$

Finally, the estimates can be expressed as [5]

$$\hat{x}_1 = x_1 + \tilde{n}_1, \quad \tilde{n}_1 \sim \mathcal{CN}(0, (1/||\mathbf{h}||_2^2)N_0) \tag{2.26}$$

$$\hat{x}_2 = x_2 + \tilde{n}_2, \quad \tilde{n}_2 \sim \mathcal{CN}(0, (1/||\mathbf{h}||_2^2)N_0) \tag{2.27}$$

where N_0 is the variance of the noise which is caused from the receiver electronics. Compared the alamouti code with transmit beamforming we conclude that Alamouti code needs double transmit power to achieve equal diversity order with the transmit beamforming method. Therefore, Alamouti code scheme lags 3dB of the transmit beamforming method.

2.3.3 Spatial Multiplexing

In spatial multiplexing systems with N_{TX} transmit antennas and N_{RX} receive antennas, a high rate data stream is spitted into multiple low rate spatial streams which transmitted from different transmit antennas. All streams transmitted over the same frequency

channel. At the receiver side is used methods to separate these data streams into parallel channels. Spatial multiplexing provides the ability increasing channel capacity at higher Signal-to-Noise Ratios (SNR). For a frequency-nonselective channel, the channel matrix $\mathbf{H}$ is expressed as

$$\begin{bmatrix} h_{11}(t) & h_{12}(t) & \dots & h_{1N_{\mathrm{TX}}}(t) \\ h_{21}(t) & h_{22}(t) & \dots & h_{2N_{\mathrm{TX}}}(t) \\ \vdots & \vdots & \ddots & \vdots \\ h_{N_{\mathrm{RX}}1}(t) & h_{N_{\mathrm{RX}}2}(t) & \dots & h_{N_{\mathrm{RX}}N_{\mathrm{TX}}}(t) \end{bmatrix} \tag{2.28}$$

The received signal at the i-th antenna is expressed as

$$r_i(t) = \sum_{j=1}^{N_{\mathrm{TX}}} h_{ij}(t)x_j(t) + n_i(t), \quad i = 1, \dots, N_{\mathrm{RX}} \tag{2.29}$$

where in matrix form is

$$\mathbf{r}(t) = \mathbf{H}(t)\mathbf{x}(t) + \mathbf{n}(t). \tag{2.30}$$

Assuming that the channel is not varying fast within a time interval $0 \leq t \leq T$ the received signal expressed simply as

$$\mathbf{r}(t) = \mathbf{H}\mathbf{x}(t) + \mathbf{n}(t), \quad 0 \leq t \leq T. \tag{2.31}$$

The equivalent discrete time equation for one symbol at the i^{th} receive antenna is

$$y_m = \sum_{n=1}^{N_{\mathrm{TX}}} s_n h_{mn} + n_m, \quad m = 1, \dots, N_{\mathrm{RX}} \tag{2.32}$$

where in matrix form is

$$\mathbf{y} = \mathbf{H}\mathbf{x} + \mathbf{n}. \tag{2.33}$$

Maximum-Likelihood Detector (MLD)

Assuming that the channel model is frequency-nonselective, and that the channel matrix $\mathbf{H}$ is known at the receiver the optimum detector for the MIMO channel model is the Maximum-Likelihood Detector (MLD). Considering that the additive noise terms at the N_{RX} antennas, are statistically independent and identically distributed (iid), zero mean Gaussian, the joint conditional PDF $p(\mathbf{y}|\mathbf{x})$ is Gaussian. Therefore, the MLD selects the symbol vector $\hat{\mathbf{x}}$ that minimizes the Euclidean distance metric

$$\mu(\mathbf{x}) = \sum_m \left| y_m - \sum_{n=1}^{N_{\mathrm{TX}}} h_{mn}x_n \right|^2 \tag{2.34}$$

with the elements of the vector $\mathbf{x}$ to belong to the constellation set $\mathcal{C}$. Thus, the complexity of the MLD method is $|\mathcal{C}|^{N_{\mathrm{TX}}}$ and increasing rapidly for large sets of constellations or large numbers of transmit antennas.

Minimum Mean Square Error Detector (MMSE)

The Minimum Mean Square Error (MMSE) approach tries to find a coefficient $\mathbf{W}$ which minimizes the mean square error,

$$J(\mathbf{W}) = E[||\mathbf{e}||_2^2] = E[||\mathbf{W}\mathbf{y} - \mathbf{x}||_2^2] \tag{2.35}$$

Solving,

$$\mathbf{W} = (\mathbf{H}^H\mathbf{H} + N_0\mathbf{I})^{-1}\mathbf{H}^H \tag{2.36}$$

The estimation of the transmitted symbols is expressed as

$$\hat{\mathbf{x}} = \mathbf{W}\mathbf{y} \tag{2.37}$$

Zero Forcing Detector (ZF)

The name Zero Forcing corresponds to bringing down the intersymbol interference (ISI) to zero in a noise free case. Zero forcing equalizer also forms an estimate of $\mathbf{x}$ by linearly combining the received signals. If $N_{\mathrm{TX}} = N_{\mathrm{RX}}$ the weighting matrix $\mathbf{W}$ is set to the inverse of channel matrix $\mathbf{W} = \mathbf{H}^{-1}$, hence

$$\hat{\mathbf{x}} = \mathbf{H}^{-1}\mathbf{y} = \mathbf{x} + \mathbf{H}^{-1}\mathbf{n} \tag{2.38}$$

When $N_{\mathrm{RX}} > N_{\mathrm{TX}}$, weighting matrix $\mathbf{W}$ may be selected as the pseudoinverse of the channel matrix

$$\mathbf{W} = \mathbf{H}^{\dagger} = (\mathbf{H}^H\mathbf{H})^{-1}\mathbf{H}^H \tag{2.39}$$

Note that the elements of vector $\mathbf{H}^{-1}\mathbf{n}$ is correlated and the decision of $\mathbf{x}$ by $\hat{\mathbf{x}}$ symbol-by-symbol is not optimum.

Chapter 3

IEEE 802.11n Physical Layer (PHY)

The 802.11n standard provides data rates up to 600Mbps. It uses the High Throughput (HT) PHY format which is based on the OFDM Non - HT PHY specification. The 802.11n is the first standard of the 802.11 series which supports MIMO scheme systems up to four spatial streams. The HT PHY data subacarriers are modulated using BPSK, QPSK, 16,64QAM. Forward Error Correction coding is used with a coding rate of ½,⅔,¾,⅚. The standard supports (as optional features) LDPC codes, short guard interval $T_{\text{SGI}} = 400ns$, transmit beamforming, the HT-greenfield format and STBC. In a HT - PHY OFDM system, the following three different formats can be supported: the Non - HT format, the HT - mixed format, and the HT - greenfield format. In this chapter, we will discuss only for the HT - mixed PPDU format. In the HT - mixed format frames, the preamble has fields that support compatibility with Non-HT STAs and fields that support HT operation. The Non-HT portion of the HT - mixed format preamble enables detection of the PPDU and acquisition of carrier frequency and timing by both HT STAs and Non-HT STAs. The standard 802.11n supports 32 different Modulation Coding Schemes (MCS) which determine the modulation, coding, and number of spatial channels, as shown in Table 3.1

Table 3.1: Modulation Coding Schemes for HT systems.

MCS	**Modulation**	**Coding Rate**	**Maximum Throughput (Mbps)**
0, 8 , 16 , 24	BPSK	1/2	60
1, 9 , 17, 25	QPSK	1/2	120
2, 10, 18, 26	QPSK	3/4	180
3, 11, 19, 27	16-QAM	1/2	240
4, 12, 20, 28	16-QAM	3/4	360
5, 13, 21, 29	64-QAM	2/3	480
6, 14, 22, 30	64-QAM	3/4	540
7, 15, 23, 31	64-QAM	5/6	600

The data rate of the system depends on the modulation coding scheme, the bandwidth, and the duration of guard interval. It can be computed from the Equation (3.1).

$$R_b = \left(R \frac{\text{info bits}}{\text{encoded bits}} \cdot N_{\text{BPSPCS}} \frac{\text{encoded bits}}{\text{symbol}} \cdot N_{\text{SD}} \frac{\text{symbols}}{\text{block}} \cdot \frac{1}{3.2\mu s + T_{\text{GI}}} \frac{\text{block}}{\text{sec}} \right) \frac{N_{\text{SS}} \text{ Spatial treams}}{\text{Spatial stream}} \tag{3.1}$$

3.1 HT - mixed PPDU Format

The HT - mixed Physical layer Protocol Data Unit (PPDU) format is presented in the Figure 3.1. HT frame consists of a legacy preamble, a HT preamble and the data portion. The legacy preamble fields are the same as the ones in Non - HT PPDU preambles. It consisting from a Legacy Short Training Field (L-STF), a Legacy Long Training Field (L-LTF), and a Legacy Signal (L-SIG) field. They allow all 802.11 devices to synchronize to the data frame, and avoid interference of other stations .The HT preamble consists a HT-SIG field, a HT - STF field , HT - LTF field and finally the data portion. The HT portion of the HT - mixed format preamble enables estimation of the MIMO channel to support demodulation of the data portion of the frame by HT STAs. The HT portion also contains the HT-SIG field that supports HT operation.

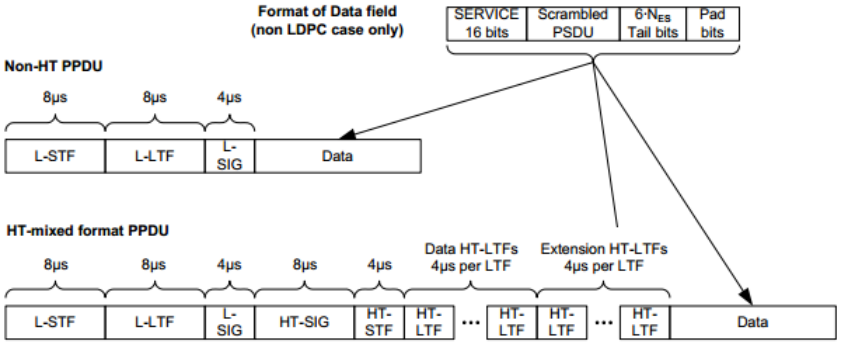

Figure 3.1: PPDU Format

3.1.1 Cyclic Shift (CS)

When the same signal or scaled copies of it, are transmitted through different transmit chains, cyclic shifts are applied to prevent unintentional beamforming. A cyclic shift of duration T_{CS} on a signal is defined as follows

$$s(t, T_{\text{CS}})\big|_{T_{\text{CS}}<0} = \begin{cases} s(t - T_{\text{CS}}) & t \in [0 \; T_{\text{CS}} + T] \\ s(t - T_{\text{CS}} - T) & t \in [T_{\text{CS}} + T \;\; T] \end{cases} \tag{3.2}$$

Equivalently, in the frequency domain, where $S(f)$ is the Fourier transform of $s(t)$, the cyclic shifted symbol can be described as

$$S_{\text{CS}}(f) = S(F)e^{-j2\pi f T_{\text{CS}}} \tag{3.3}$$

The cyclic shift is applied to each OFDM symbol in the packet separetely. Table 3.2 gives the values of the cyclic shifts that are applied to the Non - HT portion of a packet.

Table 3.2: Cyclic shifts duration duration values for non-HT portion of packet on 802.11n.

N_{TX}	T^1_{CS}	T^2_{CS}	T^3_{CS}	T^4_{CS}
1	0	-	-	-
2	0	-200ns	-	-
3	0	-100ns	-200ns	-
4	0	-50ns	-100ns	-150ns

At the HT-portion of a packet the cyclic shift duration values is given at the Table 3.3

Table 3.3: Cyclic shifts duration duration values for HT portion of packet on 802.11n.

N_{TX}	T^1_{CS}	T^2_{CS}	T^3_{CS}	T^4_{CS}
1	0	-	-	-
2	0	-400ns	-	-
3	0	-400ns	-200ns	-
4	0	-400ns	-200ns	-600ns

3.1.2 Tone Rotation

When using the 40MHz bandwidth the upper tones rotated by 90° as shown in the Figure 3.2. The mathematical representation of this rotation is given by the following function

$$Y_k = \begin{cases} 1 & k \leq 0, \text{ in a 40MHz channel} \\ j & k > 0, \text{ in a 40MHz channel} \\ 1 & \text{in a 20 MHz channel} \end{cases} \tag{3.4}$$

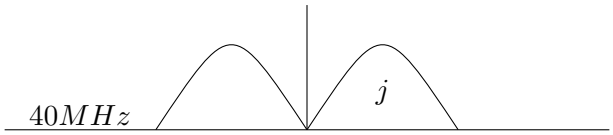

Figure 3.2: Upper tones rotation in 40MHz channel.

3.1.3 L-STF

The L-STF is used for synchronization, carrier frequency offset estimation, and automatic gain control.It consists of 10 short symbols. The non-HT short training OFDM symbol in the 20 MHz channel width is the sequence

$$\begin{aligned}\mathcal{S}_{-26:26} = \sqrt{1/2}\{&0,0,1+j,0,0,0,-1-j,0,0,0,1+j,0,0,0,-1-j,0,0,0,-1-j,0,0,0,1+j,0,\\ &0,0,0,0,0,0,-1-j,0,0,0,-1-j,0,0,0,1+j,0,0,0,1+j,0,0,0,1+j,0,0,0,1+j,0,0\}\end{aligned} \tag{3.5}$$

and in the 40 MHz channel width is the sequence

$$\mathcal{S}_{-58:58} = \{\mathcal{S}_{-26:26},0,0,0,0,0,0,0,0,0,0,0,\mathcal{S}_{-26:26}\} \tag{3.6}$$

These sequences was chosen to have good correlation properties and a low peak-to average power so that its properties are preserved even after clipping or compression by an overloaded analog front end. An IFFT creates $3.2\mu s$ time domain sequence with a pattern which repeats four times (resulting in $0.8\mu s$ periodicity). This sequence may then be repeated

two and half times to create ten short symbol repetitions. The L-STF signal on transmit chain i_{TX} is :

$$r_{\mathrm{L-STF}}^{(i_{\mathrm{TX}})}(t) = \frac{1}{\sqrt{N_{\mathrm{L-STF}}^{\mathrm{Tone}} \cdot N_{\mathrm{TX}}}} W_{T_{\mathrm{L-STF}}}(t) \sum_{k=-N_{\mathrm{SR}}}^{N_{\mathrm{SR}}} Y_k S_k^{i_{\mathrm{TX}}} e^{j2\pi k \Delta_F (t - T_{\mathrm{CS}}^{i_{\mathrm{TX}}})} \tag{3.7}$$

where N_{SR} is the highest data subcarrier index and the $1/\left(\sqrt{N_{\mathrm{L-STF}}^{\mathrm{Tone}} \cdot N_{\mathrm{TX}}}\right)$ scale factor ensures that the total power of the time domain signal as summed over all transmit chains is either 1.

3.1.4 L-LTF

The L-LTF consists two long training symbols and is used for the channel and fine frequency carrier offset estimation. A long training symbol in 20MHz channel bandwidth consists of 53 subcarriers (including the value 0 at DC) which are modulated by the elements of the sequence $\mathcal{L}$ given by

$$\begin{aligned}\mathcal{L}_{-26:26} =& \{1, 1, -1, -1, 1, 1, -1, 1, -1, 1, 1, 1, 1, 1, 1, -1, -1, 1, 1, -1, 1, -1, 1, 1, 1, 1, 0, \\ & 1, -1, -1, 1, 1, -1, 1, -1, 1, -1, -1, -1, -1, -1, 1, 1, -1, -1, 1, -1, 1, -1, 1, 1, 1, 1\}\end{aligned} \tag{3.8}$$

For the 40MHz bandwidth the long training symbols is constructed of repeated copies of the sequence $\mathcal{L}$ as shown in Equation (3.9). Before L-LTF field inserted double guard interval ($T_{\mathrm{GI2}} = 1.6\mu s$).

$$\mathcal{L}_{-58:58} = \{\mathcal{L}_{-26:26}, 0, 0, 0, 0, 0, 0, 0, 0, 0, 0, 0, \mathcal{L}_{-26:26}\} \tag{3.9}$$

The time domain signal on transmit chain i_{tx} of a long training symbol is given by the equation

$$r_{\mathrm{L-LTF}}^{(i_{\mathrm{TX}})}(t) = \frac{1}{\sqrt{N_{\mathrm{L-LTF}}^{\mathrm{Tone}} \cdot N_{\mathrm{TX}}}} W_{T_{\mathrm{L-LTF}}}(t) \sum_{k=-N_{\mathrm{SR}}}^{N_{\mathrm{SR}}} Y_k L_k^{i_{\mathrm{TX}}} e^{j2\pi k \Delta_F (t - T_{\mathrm{GI2}} - T_{\mathrm{CS}}^{i_{\mathrm{TX}}})} \tag{3.10}$$

3.1.5 L-SIG

The L-SIG field is used to encode the rate and length data bits information. The structure of the L-SIG is shown in Figure 3.3.

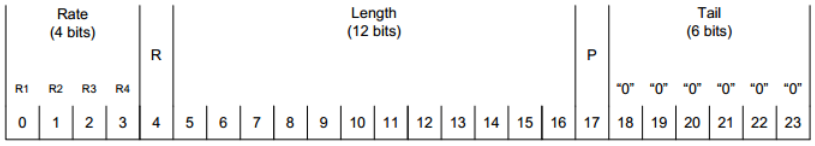

Figure 3.3: The structure of legacy signal field.

The rate field conveys information about the type of modulation and coding rate in Non-HT systems. At the HT-mixed OFDM system the rate field is set it always to '1101'. At the length field we set a 12 bit unsigned integer that indicates the number of octets in the PSDU. The reserved bit R it shall be set to 0, and the parity bit stores the even parity of first 17 bits (bits 0-16). Finally the tail bits are set it to zeros. The coding of the L-SIG single OFDM symbol shall be performed with BPSK modulation of the subcarriers and using convolutional coding at $R = 1/2$. The encoding procedure, includes convolutional coding, interleaving,modulation mapping processes , pilot insertion and OFDM modulation. Since coding rate $R = 1/2$ and the modulation that used is BPSK the 24 bits mapped to 48 complex symbols at the frequency. In 20 MHz transmission the time domain waveform of the L-SIG given by the equation

$$r^{i_{\mathrm{TX}}}_{\mathrm{L-SIG}}(t) = \frac{1}{\sqrt{N^{\mathrm{Tone}}_{\mathrm{L-SIG}} \cdot N_{\mathrm{TX}}}} W_{T_{\mathrm{SYM}}}(t) \sum_{k=-26}^{26} (D_k + p_0 P_k) e^{j2\pi k \Delta_F (t - T_{\mathrm{GI}} - T^{i_{\mathrm{TX}}}_{\mathrm{CS}})} \tag{3.11}$$

and in a 40 MHz transmission the time domain waveform is

$$r^{i_{\mathrm{TX}}}_{\mathrm{L-SIG}}(t) = \frac{1}{\sqrt{N^{\mathrm{Tone}}_{\mathrm{L-SIG}} \cdot N_{\mathrm{TX}}}} W_{T_{\mathrm{SYM}}}(t) \sum_{k=-26}^{26} (D_k + p_0 P_k) \left(e^{j2\pi(k-32)\Delta_F (t - T_{\mathrm{GI}} - T^{i_{\mathrm{TX}}}_{\mathrm{CS}})} + j e^{j2\pi(k+32)\Delta_F (t - T_{\mathrm{GI}} - T^{i_{\mathrm{TX}}}_{\mathrm{CS}})} \right) \tag{3.12}$$

where

$$D_k = \begin{cases} 0 & k = \pm 21, \pm 7 \\ d_{M^r(k)} & \text{otherwise} \end{cases} \tag{3.13}$$

, $M^r(k)$ is given by the form

$$M^r(k) = \begin{cases} k + 26, & -26 \le k \le -22 \\ k + 25, & -20 \le k \le -8 \\ k + 24, & -6 \le k \le -1 \\ k + 23, & 1 \le k \le 6 \\ k + 22, & 8 \le k \le 20 \\ k + 21, & 22 \le k \le 26 \end{cases} \tag{3.14}$$

and the p_0 value, and P_k sequence, constitute the pilot signals sequence.

3.1.6 HT-SIG

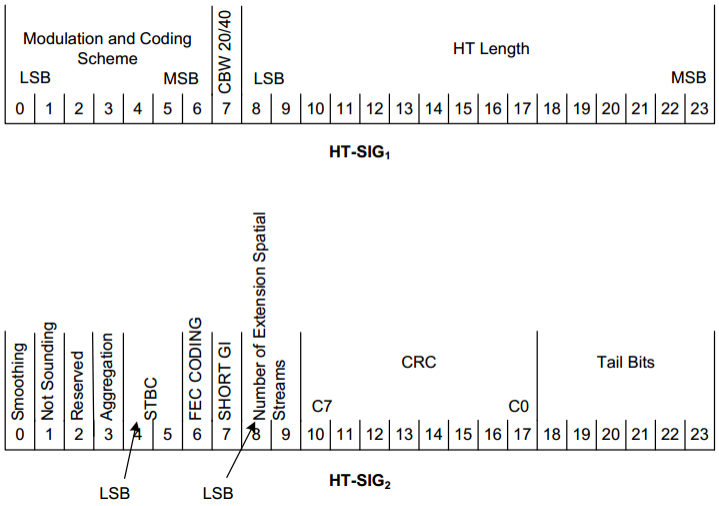

Figure 3.4: HT-SIG structure

The HT-SIG is the first HT field, it consists of two symbols that carries parameters(Figure 3.4) for an 802.11n station to decode the rest of the signal. The HT-SIG consistss of two symbols each containing 24 bits. The HT-SIG1 communicate information about the channel bandwidth, the Modulation Coding Scheme, and the the number of octets of data in the PSDU. The second symbol HT-SIG2 contains information about optional features as STBC, short GI, LDPC coding etc. Also contains 8 bits on the field CRC to detect errors on the first 34 bits of HT-SIG field. The HT-SIG parts shall be encoded a $R = 1/2$, interleaved, and mapped to a BPSK constellation. The BPSK constellation is rotated by 90° relative to the L-SIG in order to accommodate detection of the start of the HT-SIG. The last 6 bits which constitute the Tail bits, are used to terminate the trellis of the convolution coder. The cyclic redundancy check (CRC) protects bits 0-33 of the HT-SIG. The value of the CRC field shall be the ones complement of

$$crc(D) = (M(D) \oplus I(D))D^8 \bmod G(D) = c_0 D^7 + \cdots + c_7. \tag{3.15}$$

where $M(D) = m_0 D^{33} + \cdots + m_{33}$ is the HT-SIG representing as polynomial with m_0 the bit 0 of HT-SIG1. $I(D) = \sum_{i=26}^{33} D^i$ are initialization values that are added modulo 2 to the first 8 bits of HT-SIG1, and $G(D) = D^8 + D^2 + D + 1$ is the CRC generating polynomial.

The time domain waveform for the 20MHz transmissions is:

$$r^{i_{\mathrm{TX}}}_{\mathrm{HT-SIG}}(t) = \frac{1}{\sqrt{N^{\mathrm{Tone}}_{\mathrm{HT-SIG}} \cdot N_{\mathrm{TX}}}} \sum_{n=0}^{1} W_{T_{\mathrm{SYM}}}(t - nT_{\mathrm{SYM}}) \sum_{k=-26}^{26} (jD_k + p_{n+1}P_k) e^{j2\pi k\Delta_F (t - nT_{\mathrm{SYM}} - T_{\mathrm{GI}} - T^{i_{\mathrm{TX}}}_{\mathrm{CS}})} \quad (3.16)$$

and in 40MHz operation is:

$$r^{i_{\mathrm{TX}}}_{\mathrm{HT-SIG}}(t) = \frac{1}{\sqrt{N^{\mathrm{Tone}}_{\mathrm{HT-SIG}} \cdot N_{\mathrm{TX}}}} \sum_{n=0}^{1} W_{T_{\mathrm{SYM}}}(t - nT_{\mathrm{SYM}}) \sum_{k=-26}^{26} (jD_k + p_{n+1}P_k)(e^{j2\pi(k-32)\Delta_F (t - nT_{\mathrm{SYM}} - T_{\mathrm{GI}} - T^{i_{\mathrm{TX}}}_{\mathrm{CS}})} + je^{j2\pi(k+32)\Delta_F (t - nT_{\mathrm{SYM}} - T_{\mathrm{GI}} - T^{i_{\mathrm{TX}}}_{\mathrm{CS}})}) \quad (3.17)$$

3.1.7 HT-STF

HT-STF field used to improve automatic gain control estimation in MIMO system. HT-STF consists of one OFDM symbol which lasts $4\mu s$ and the subcarrier frequency sequence is identical to that of the L-STF, defined in Equation (3.5) for 20MHz transmission and in Equation (3.6) for 40MHz transmission. The time domain equation of the HT-STF field is expressed as

$$r^{i_{\mathrm{TX}}}_{\mathrm{HT-STF}}(t) = \frac{1}{\sqrt{N^{\mathrm{Tone}}_{\mathrm{HT-STF}} \cdot N_{\mathrm{TX}}}} W_{T_{\mathrm{HT\text{-}STF}}}(t) \sum_{k=-N_{\mathrm{SR}}}^{N_{\mathrm{SR}}} \sum_{i_{\mathrm{STS}}=1}^{N_{\mathrm{STS}}} [Q_k]_{i_{\mathrm{TX}}, i_{\mathrm{STS}}} Y_k \mathrm{HT-STF}_k e^{j2\pi k\Delta_F (t - T^{i_{\mathrm{STS}}}_{\mathrm{CS}})} \quad (3.18)$$

where Q_k is the spatial mapping matrix which maps fewer spatial streams to more transmit antennas if needed.

3.1.8 HT-LTF

The HT-LTF is used by the receiver for MIMO channel estimation, and equalizing the DATA fields. The HT-LTF portion has one or two parts, where the first part consits of one, two or four HT-DTLFs that are necessary for demodulation of the HT-Data portion of the PPDU. The second part is optional and constructed from HT-LTFs that are referred as

HT-ELTFs. Assuming that N_{HTDLTF} is the number of training symbols consisting the first part and N_{STS} the number of space-time streams, the number N_{HTDLTF} can be expressed as

$$N_{\mathrm{HTDLTF}} = \begin{cases} N_{\mathrm{STS}}, & \text{if } N_{\mathrm{STS}} = 1, 2, 4 \\ 4, & \text{if } N_{\mathrm{STS}} = 3 \end{cases} \tag{3.19}$$

The number of optional training symbols HT-ELTFs N_{HTELTF} is depended on the number of extension spatial streams N_{ESS}.

$$N_{\mathrm{HTELTF}} = \begin{cases} 0, & \text{if } N_{\mathrm{ESS}} = 0 \\ N_{\mathrm{ESS}}, & \text{if } N_{\mathrm{ESS}} = 1, 2 \\ 4, & \text{if } N_{\mathrm{ESS}} = 3 \end{cases} \tag{3.20}$$

Since $N_{\mathrm{STS}} + N_{\mathrm{ESS}} \leq 4$, the total number of HT-LTFs $N_{\mathrm{HTLTF}} = N_{\mathrm{HTDLTF}} + N_{\mathrm{HTELTF}} \leq 5$

An orthogonal mapping matrix is used to generate the HT-LTF. The HT long training frequency sequence is multiplied by a value (+1 or -1) from the orthogonal mapping matrix

$$P = \begin{bmatrix} 1 & -1 & 1 & 1 \\ 1 & 1 & -1 & 1 \\ 1 & 1 & 1 & -1 \\ -1 & 1 & 1 & 1 \end{bmatrix}. \tag{3.21}$$

The HT long training symbol for 20 MHz operation is defined based on the frequency domain sequence $\mathcal{L}$

$$\mathrm{HTLTF}_{-28:28} = \{1, 1, \mathcal{L}_{-26:26}, -1, -1\}. \tag{3.22}$$

and for 40 MHz operation the corresponding sequence defined based on the $\mathcal{L}_{-58:58}$ by filling the missing subcarriers $[-32, -5, -4, -3, -2, 2, 3, 4, 5, 32]$ with the values $[1, -1, -1, -1, 1, -1, 1, 1, -1, 1]$. The time domain representation of the waveform transmitted on transmit chain during HT-DLTF n, where $1 \leq n \leq N_{\mathrm{HTDLTF}}$ shall be as shown in equation

$$r_{\mathrm{HT-LTF}}^{n,i_{\mathrm{TX}}}(t) = \frac{1}{N_{\mathrm{STS}} \cdot N_{\mathrm{HT-LTF}}^{\mathrm{Tone}}} W_{T_{\mathrm{HT-LTFs}}}(t) \sum_{k=-N_{\mathrm{SR}}}^{N_{\mathrm{SR}}} \sum_{i_{\mathrm{STS}}=1}^{N_{\mathrm{STS}}} [Q_k]_{i_{TX}, i_{\mathrm{STS}}} [P_{\mathrm{HTLTF}}]_{i_{\mathrm{STS}}, n} Y_k \mathrm{HTLTF}_k e^{j2\pi k \Delta_F (t - T_{\mathrm{GI}} - T_{\mathrm{CS}}^{i_{\mathrm{STS}}})}. \tag{3.23}$$

For the HT-ELTFs ($N_{\mathrm{HTDLTF}} < n \leq N_{\mathrm{HTLTF}}$) , it shall be as shown in the following equation

$$r_{HT-LTF}^{n,i_{\mathrm{TX}}}(t) = \frac{1}{N_{\mathrm{ESS}} \cdot N_{\mathrm{HT-LTF}}^{\mathrm{Tone}}} W_{T_{\mathrm{HT-LTFs}}}(t) \sum_{k=-N_{\mathrm{SR}}}^{N_{\mathrm{SR}}} \sum_{i_{\mathrm{ESS}}=1}^{N_{\mathrm{ESS}}} [Q_k]_{i_{\mathrm{TX}}, N_{\mathrm{STS}} + i_{\mathrm{STS}}} [P_{\mathrm{HTLTF}}]_{i_{\mathrm{ESS}}, n - N_{\mathrm{HTDLTF}}} Y_k \mathrm{HTLTF}_k e^{j2\pi k \Delta_F (t - T_{\mathrm{GI}} - T_{\mathrm{CS}}^{i_{\mathrm{ESS}}})} \tag{3.24}$$

where $P_{\text{HTLTF}} = P$ as defined in Equation (3.21).

3.1.9 Data Field

When BCC encoding is used, the Data field consists of the 16-bit Service field, the PSDU, either six or twelve tail bits depending on wether one or two encoding streams are represented, and pad bits. The number of pad bits is adaptive in order that the total number of bits in the Data field to be an integer multiple of OFDM symbols. The number of OFDM symbols in the Data field when BCC encoding is used it can be computed as follows

$$N_{\text{SYM}} = m_{\text{STBC}} \left\lceil \frac{8 \cdot \text{length} + 16 + 6 \cdot N_{ES}}{m_{\text{STBC}} \cdot N_{\text{DBPS}}} \right\rceil \tag{3.25}$$

where N_{DBPS} is the number of data bits per OFDM symbol determined by the selected MCS, length is the value of the Length field in octets in the HT-SIG, and m_{STBC} is 2 if STBC is used (to ensure that we will have even number of bits) and 1 otherwise. The number of pad bits is therefore

$$N_{\text{PAD}} = N_{\text{SYM}} \cdot N_{\text{DBPS}} - 8 \cdot \text{length} - 16 - 6 \cdot N_{\text{ES}} \tag{3.26}$$

The Service field of HT Data portion consisting of 16 zero bits that used to initialize the Scrambler.

3.2 Transmitter Structure

In this section it will be analyzed the procedure on transmitter for the HT-Data field. The transmitter structure is presented in the Figure 3.5.

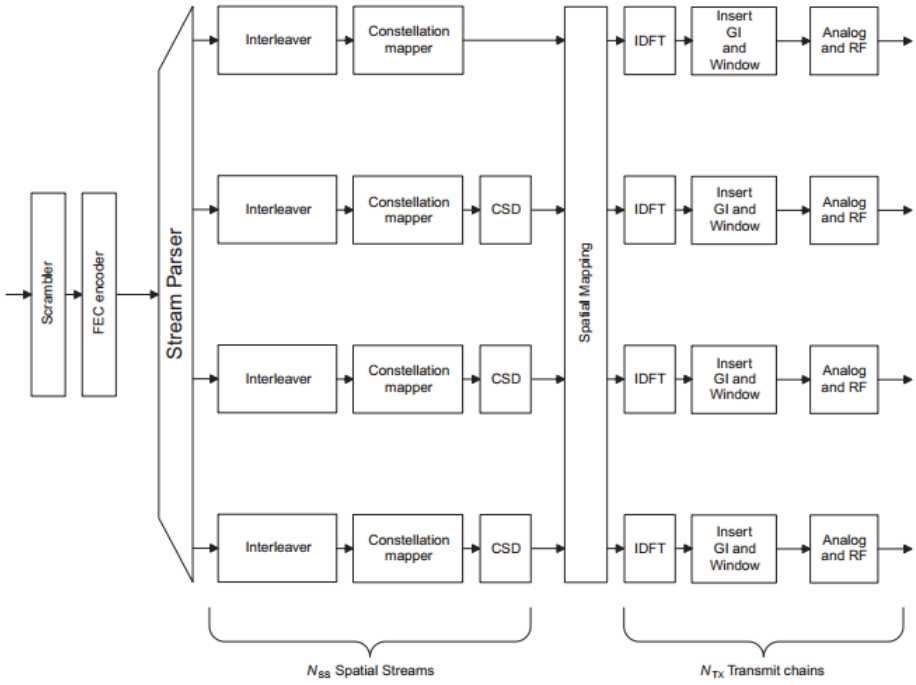

Figure 3.5: Transmitter Structure ([6])

3.2.1 Scrambler

The scrambler takes as input a stream of bits on which apply shifts and xor operations in order that the output stream is free of long sequences of bits with the same value. Only the Data field is being scrambled. The frame-synchronous scrambler has the advantage that only one transmission error is produced from a single error after receiver descrambler. The structure of scrambler is presented in Figure 3.6 and initialized with an integer in the interval [1 127]. The frame-synchronous generator polynomial is given by

$$S(x) = x^7 + x^4 + 1 \tag{3.27}$$

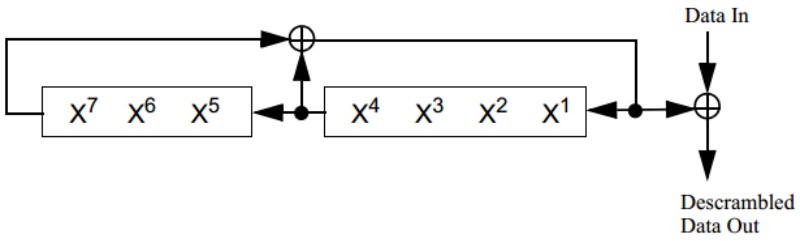

Figure 3.6: Scrambler structure.

At the receiver, the first seven bits of the Service field give the initial state of the scrambler. To descramble the receive data we use the same structure.

3.2.2 Forward Error Correction Code (FEC)

The HT PHY OFDM system supports two different Forward Error Correction code encoders, the Binary Convolutional Code (BCC) and the LDPC. In this thesis we will not discuss for the LDPC encoder. The Data Field shall be coded with a convolutional encoder of coding rate R = 1/2, 2/3,3/4 or 5/6 accordingly to the modulation coding scheme being used. The convolutional encoder shall use the industry - standard generator polynomials , $g_0 = 133_8$ and $g_1 = 171_8$ of rate $R = 1/2$. Higher rates are derived from it by employing puncturing, that is, bits are removed from the encoded sequence (with rate $R = 1/2$) to achieve a larger coding rate. At the receiver side, dummy zero bits are inserted in the decoder to replace the removed bits.

BCC Encoder Parser

In 802.11n two BCC encoders have to be used simultaneously to handle the encoding process at high data rates. Single encoder is used when LDPC coding used or when the BCC encoder used with data rate $\leq$ 300Mbps. For data rates greater than 300Mbps two BCC encoders are used. In this case an encoder parser is needed to divide the scrambled bits among to the two BCC encoders in a round-robin scheduling fashion. Note that the data rate is dependent from the MCS, the bandwidth, the duration of guard interval and the number of spatial streams. Bit with index i sent to the encoder j, denoted $x_i^{(j)}$ is shown in the following equation.

$$x_i^{(j)} = b_{N_{\mathrm{ES}} \cdot i + j}, \quad 0 \leq j \leq N_{\mathrm{ES}} - 1 \tag{3.28}$$

Following the parsing operation, 6 scrambled zero bits following the end of the message bits in each BCC input sequence are replaced by unscrambled zero bits.

3.2.3 Stream Parser

Stream parser divides the encoded streams of each encoder into N_{SS} new bit strings, each of length N_{CBPSS} (coded bits per spatial stream). Consecutive blocks of bits are assigned to different spatial streams in a round robin fashion. The number of bits assigned to a single axis in a constellation point in spatial stream i_{SS} is denoted by the following equation

$$s(i_{\mathrm{SS}}) = max\left\{1, \frac{N_{\mathrm{BPSCS}}}{2}\right\} \tag{3.29}$$

where N_{BPSCS} is the modulation order. The sum of these over all streams is

$$S = \sum_{i_{\mathrm{SS}}=1}^{N_{\mathrm{SS}}} s(i_{\mathrm{SS}}) \tag{3.30}$$

If all spatial streams modulated with the same MCS then $S = N_{\mathrm{SS}} \cdot s$. Input k to spatial stream i_{SS} shall be $y_i^{(j)}$, which is output bit i of the encoder j, where

$$j = \left\lfloor \frac{k}{s(i_{\mathrm{SS}})} \right\rfloor \bmod N_{\mathrm{ES}} \tag{3.31}$$

$$i = \sum_{i'=1}^{i_{\mathrm{SS}}-1} s(i') + S \left\lfloor \frac{k}{N_{\mathrm{ES}} \cdot s(i_{\mathrm{SS}})} \right\rfloor + k \bmod s(i_{\mathrm{SS}}) \tag{3.32}$$

The output of the parser is

$$x_k^{i_{\mathrm{SS}}} = y_i^{(j)}, \quad 1 \le i_{\mathrm{SS}} \le N_{\mathrm{SS}},\ k = 0, 1, \ldots, N_{\mathrm{CBPSS}} - 1 \tag{3.33}$$

Figure 3.7 illustrates an example of single encoder, equal MCS, 64-QAM(s=3) and 3 spatial streams.

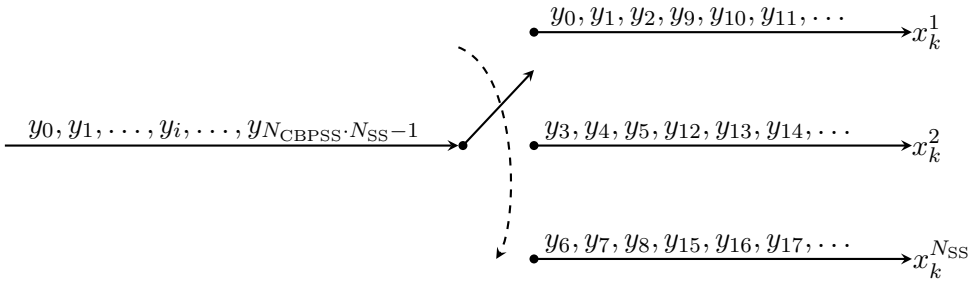

Figure 3.7: Stream parser for single encoder and equal MCS.

3.2.4 Frequency Interleaver

The use of interleaver structure in systems where is also used error correction codes is very important as increases the performance by achieving time diversity without decreasing the data rate. Wireless channels are having statistical dependence among successive transmission of symbols that results in errors in bursts. Also is well known that a code word with a burst error of length greater than the BCCs error correction capability it can't be recovered at receiver. Interleaving helps overcoming this problem by shuffling the data bits in different code words creating a better uniform distribution of the errors. Thus, the probability of not being able the error correction code to recover a code word decreases. The interleaver of HT OFDM system applies the three following permutations, which dependent on the parameters showing in Table 3.4

- The first permutation ensures that adjacent coded bits are mapped onto non-adjacent subcarriers.

$$i = N_{\mathrm{ROW}}(k \bmod N_{\mathrm{COL}}) + \left\lfloor \frac{k}{N_{\mathrm{COL}}} \right\rfloor, \quad k = 0, \ldots, N_{\mathrm{CBPSS}}(i_{\mathrm{SS}}) - 1 \tag{3.34}$$

- The second permutation ensures that adjacent coded bits are mapped alternately onto less and more significant bits of the constellation, avoiding long runs of low reliability bits.

$$j = s(i_{\mathrm{SS}}) \cdot \left\lfloor \frac{i_{\mathrm{SS}}}{s(i_{\mathrm{SS}})} \right\rfloor + \left(i + N_{\mathrm{CBPSS}}(i_{\mathrm{SS}}) - \left\lfloor N_{\mathrm{COL}} \frac{i}{N_{\mathrm{CBPSS}}(i_{\mathrm{SS}})} \right\rfloor \bmod s(i_{\mathrm{SS}}) \right), \quad i = 0, \ldots, N_{\mathrm{CBPSS}}(i_{\mathrm{SS}}) - 1 \tag{3.35}$$

- If more than one spatial stream exists, the third operation is applied, which performs a frequency rotation to the additional spatial streams.

$$r = \left(j - \left((2(i_{\mathrm{SS}} - 1)) \bmod 3 + 3 \left\lfloor \frac{i_{\mathrm{SS}} - 1}{3} \right\rfloor \cdot N_{\mathrm{ROT}} \cdot N_{\mathrm{BPSCS}}(i_{\mathrm{SS}}) \right) \right) \bmod N_{\mathrm{CBPSS}}(i_{\mathrm{SS}}), \quad j = 0, \ldots, N_{\mathrm{CBPSS}}(i_{\mathrm{SS}}) - 1 \tag{3.36}$$

Finally the outputs of the interleaver are

$$z_k^{i_{\mathrm{SS}}} = x_r^{i_{\mathrm{SS}}}, \quad 1 \le i_{\mathrm{SS}} \le N_{\mathrm{SS}},\, r = 0, \ldots, N_{\mathrm{CBPSS}}(i_{\mathrm{SS}}) - 1 \tag{3.37}$$

Table 3.4: Block interleaver parameters.

Parameter	**20MHz**	**40MHz**
$\mathbf{N}_{\mathrm{COL}}$	13	18
$\mathbf{N}_{\mathrm{ROW}}$	$4 \cdot N_{\mathrm{BPSCS}}(i_{\mathrm{SS}})$	$6 \cdot N_{\mathrm{BPSCS}}(i_{\mathrm{SS}})$
$\mathbf{N}_{\mathrm{ROT}}$	11	29

3.2.5 Constellation Mapper

The encoded and interleaved bit streams are divided into groups of length N_{BPSC}(number of bits per subcarrier) and are mapped into complex numbers representing any of 4 different constellations that are being used. The first $N_{\mathrm{BPSC}}/2$ bits of each group are mapped into a point on the inphase axis and the last $N_{\mathrm{BPSC}}/2$ into a point on the quadrature axis respectively. The constellations are Grey-coded and normalized by the factor K_{MOD} which depends on the modulation mode and ensures that all mappings will achieve the same average power. The purpose of using the Grey code is to increase the performance of the system. In a false decision of a symbol at the receiver, with high probability the decided false symbol is adjacent to the true. Therefore, in this case, with the usage of Grey code is being ensured that only one bit error will occur. The streams of the complex numbers are denoted as shown below

$$d_{k,l,n}, \quad 0 \le k \le N_{\mathrm{SD}} - 1, \quad 1 \le l \le N_{\mathrm{SS}}, \quad 0 \le n \le N_{\mathrm{SYM}} - 1 \tag{3.38}$$

Table 3.5: Normalization factor number K_{MOD} for the different modulations.

Modulation	$\mathbf{K}_{\text{MOD}}$
BPSK	1
QPSK	$1/\sqrt{2}$
16-QAM	$1/\sqrt{10}$
64-QAM	$1/\sqrt{42}$

3.2.6 STBC

Space time block coding can be used optionally if the number of space-time streams is greater that the number of spatial streams. Using the STBC transmission format, the N_{SS} spatial streams are mapped to N_{STS} space time streams, which are mapped to N_{TX} transmit chains. Additionally, STBC is a method to achieve higher diversity order increasing the performance of the system. For more details see section 2.3.2. If STBC applied, the stream of complex numbers $d_{k,l,n}$ is given as input to STBC encoder, which produces the output stream $\tilde{d}_{k,i,n}$ of complex numbers.

$$\tilde{d}_{k,i,n}, \quad 0 \leq k \leq N_{\text{SD}} - 1, \quad 1 \leq i \leq N_{\text{STS}}, \quad 0 \leq n \leq N_{\text{SYM}} - 1 \tag{3.39}$$

The transformations of the stream d to the stream $\tilde{d}$ which are supported from 802.11n standard presented in [6] (Table 20-18).

3.2.7 Pilots Insertion

Pilot signals are inserted to each OFDM symbol to make the coherent detection robust against frequency offsets and phase noise. Pilot subcarriers are scattered to the frequency bandwidth so that there is the possibility of estimation in the whole spectrum used. In 802.11n 20 MHz operation 4 subcarriers are dedicated to pilot signals and in 40MHz operation 6 pilot subcarriers. The pilot sequence for the n^{th} OFDM symbol and i^{th} space - time stream is the $P_{i_{\text{STS}},n}^{-28:28}$ in a 20MHz transmission and the $P_{i_{\text{STS}},n}^{-58:58}$ in a 40MHz transmission. These sequences have non zero values only in the pilot subcarriers indices as shown in Table 3.6. For each spatial stream there is a different pilot subcarrier pattern. In addition, for each number of spatial streams, the set of pilot subcarrier patterns is different. And finally, the pattern is cyclically shifted from symbol to symbol(for more details [6]).

Table 3.6: Pilot Subcarriers indeces in 802.11n.

Bandwidth	**Subcarriers indeces**
20MHz	$[-21 \quad -7 \quad 7 \quad 21]$
40MHz	$[-53 \quad -25 \quad -11 \quad 11 \quad 25 \quad 53]$

3.2.8 Spatial Mapping

Spatial mapper is used to rotate or scale the constellation mapper output vector. The spatial mapper expands the space-time streams into a number of transmit chains N_{TX}, if not used then N_{TX} will be equal to N_{STS} and every space-time stream is transmitted through a separate antenna. It could also be used to simply duplicate the space-time streams to utilise more antennas, expanding the N_{STS} into a larger N_{TX}. Spatial mapping is represented by the spatial mapping matrix Q_k. The spatial mapping matrix have N_{TX} rows and N_{STS} columns for subcarrier k. Some examples is given below

Direct Mapping

In the case of direct mapping, the number of space-time streams is equal to the number of transmit chains. Q_k is a diagonal matrix of unit magnitude complex values that takes one of two forms:

- $Q_k = \mathbf{I}$, the identity matrix.
- A CSD matrix in which the diagonal elements represent shifts in the time-domain: $[Q_k]_{(i,i)} = e^{-j2\pi k \Delta_F \tau^i_{\mathrm{CS}}}$, where $\tau^i_{\mathrm{CS}}, i = 1, \ldots, N_{\mathrm{TX}}$ represents the CSD applied.

Indirect Mapping

Hadamard matrix or the Fourier matrix used for indirect mapping. The Hadamard mapping matrix is of size $N_{\mathrm{TX}} \times (N_{\mathrm{STS}} + N_{\mathrm{ESS}})$, where $N_{\mathrm{TX}} \geq (N_{\mathrm{STS}} + N_{\mathrm{ESS}})$. The Hadamard mapping matrix is derived by taking subset of the 8×8 Hadamard matrix. An example of 4×4 Hadamard matrix is

$$Q_k = \frac{1}{2} \begin{bmatrix} 1 & 1 & 1 & 1 \\ 1 & -1 & 1 & -1 \\ 1 & 1 & -1 & -1 \\ 1 & -1 & -1 & 1 \end{bmatrix} \tag{3.40}$$

The element in n^{th} row and m^{th} column of the Fourier matrix with dimensions $N_{\mathrm{TX}} \times N_{\mathrm{STS}} + N_{\mathrm{ESS}}$ is

$$a_{n,m} = \frac{1}{\sqrt{N_{\mathrm{TX}}}} e^{\frac{j2\pi(m-1)(n-1)}{N_{\mathrm{TX}}}}, \quad n = 1, \ldots, N_{\mathrm{TX}}, m = 1, \ldots, N_{\mathrm{STS}} + N_{\mathrm{ESS}} \tag{3.41}$$

An example of 2×1 matrix, for a MISO system is

$$Q_k = \frac{1}{\sqrt{2}} \begin{bmatrix} 1 \\ 1 \end{bmatrix} \tag{3.42}$$

Spatial Expansion

Q_k is the product of a CSD matrix and a square matrix formed of orthogonal columns. Spatial Expansion may be performed by duplicating some of the N_{STS} streams to form the N_{TX} streams, with each stream being scaled by the normalization factor $\sqrt{N_{\mathrm{STS}}/N_{\mathrm{TX}}}$.

$$Q_k = M_{\mathrm{CSD}}(k) \cdot D \tag{3.43}$$

where $M_{\mathrm{CSD}}(k)$ is a CSD, matrix or any unitary matrix. Some examples of the matrix D are

$$N_{\mathrm{TX}} = 4, N_{\mathrm{STS}} = 1, \quad D = \frac{1}{2}\begin{bmatrix}1 & 1 & 1 & 1\end{bmatrix}^T \tag{3.44}$$

$$N_{\mathrm{TX}} = 3, N_{\mathrm{STS}} = 2, \quad D = \sqrt{\frac{2}{3}}\begin{bmatrix}1 & 0\\ 0 & 1\\ 1 & 0\end{bmatrix}^T \tag{3.45}$$

If $M_{\mathrm{CSD}}(k)$ is a CSD matrix and $N_{\mathrm{TX}} = 4, N_{\mathrm{STS}} = 1$, the matrix Q_k is

$$Q_k = M_{\mathrm{CSD}}(k) \cdot D = \begin{bmatrix}1 & 0 & 0 & 0\\ 0 & e^{-j2\pi k\Delta_F \tau_{\mathrm{CS}}^2} & 0 & 0\\ 0 & 0 & e^{-j2\pi k\Delta_F \tau_{\mathrm{CS}}^3} & 0\\ 0 & 0 & 0 & e^{-j2\pi k\Delta_F \tau_{\mathrm{CS}}^4}\end{bmatrix}\frac{1}{2}\begin{bmatrix}1\\1\\1\\1\end{bmatrix} =$$

$$= \frac{1}{2}\begin{bmatrix}1\\ e^{-j2\pi k\Delta_F \tau_{\mathrm{CS}}^2}\\ e^{-j2\pi k\Delta_F \tau_{\mathrm{CS}}^3}\\ e^{-j2\pi k\Delta_F \tau_{\mathrm{CS}}^4}\end{bmatrix}$$

3.2.9 Transmission in HT format

For 20 MHz HT transmissions, the signal from transmit chain $i_{\mathrm{TX}}, 1 \le i_{\mathrm{TX}} \le N_{\mathrm{TX}}$ shall be as shown in the following equation

$$r_{\text{HT-DATA}}^{i_{\mathrm{TX}}}(t) = \frac{1}{\sqrt{N_{\mathrm{STS}} \cdot N_{\text{HT-DATA}}^{\mathrm{Tone}}}} \sum_{n=0}^{N_{\mathrm{SYM}}-1} W_{T_{\mathrm{SYM}}}(t - nT_{\mathrm{SYM}})$$
$$\sum_{k=-N_{\mathrm{SR}}}^{N_{\mathrm{SR}}} \sum_{i_{\mathrm{STS}}=1}^{N_{\mathrm{STS}}} ([Q_k]_{i_{\mathrm{TX}},i_{\mathrm{STS}}}(\tilde{D}_{k,i_{\mathrm{STS}}}, n + p_{n+z}P^k_{i_{\mathrm{STS}},n}))e^{j2\pi k\Delta_F(t - nT_{\mathrm{SYM}} - T_{\mathrm{GI}} - T_{\mathrm{CS}}^{i_{\mathrm{STS}}})} \tag{3.46}$$

where z = 3 in a HT-mixed format packet, and

$$\tilde{D}_{k,i_{\mathrm{STS}},n}\begin{cases} 0 & k = \pm 21, \pm 7\\ \tilde{d}_{M^r(k),i_{\mathrm{STS}},n} & \text{otherwise}\end{cases} \tag{3.47}$$

3.3 Receiver Structure

The receiver first must estimate and correct for the frequency offset and the symbol timing by using the training symbols in the preamble. Subsequently, the CP is removed, and the N_{FFT} point discrete fourier transformation (DFT) is performed per receiver branch. Since the MIMO algorithms as proposed in section 2.3 are single carrier algorithms, MIMO detection has to be done per OFDM subcarrier. Therefore, the received signals of subcarrier k are routed to the k^{th} MIMO detector to recover the N_{SS} data signals transmitted on that subcarrier. Next, the symbols per N_{SS} stream are combined, and finally, demapping, deinterleaving , decoding and descrambling are performed.

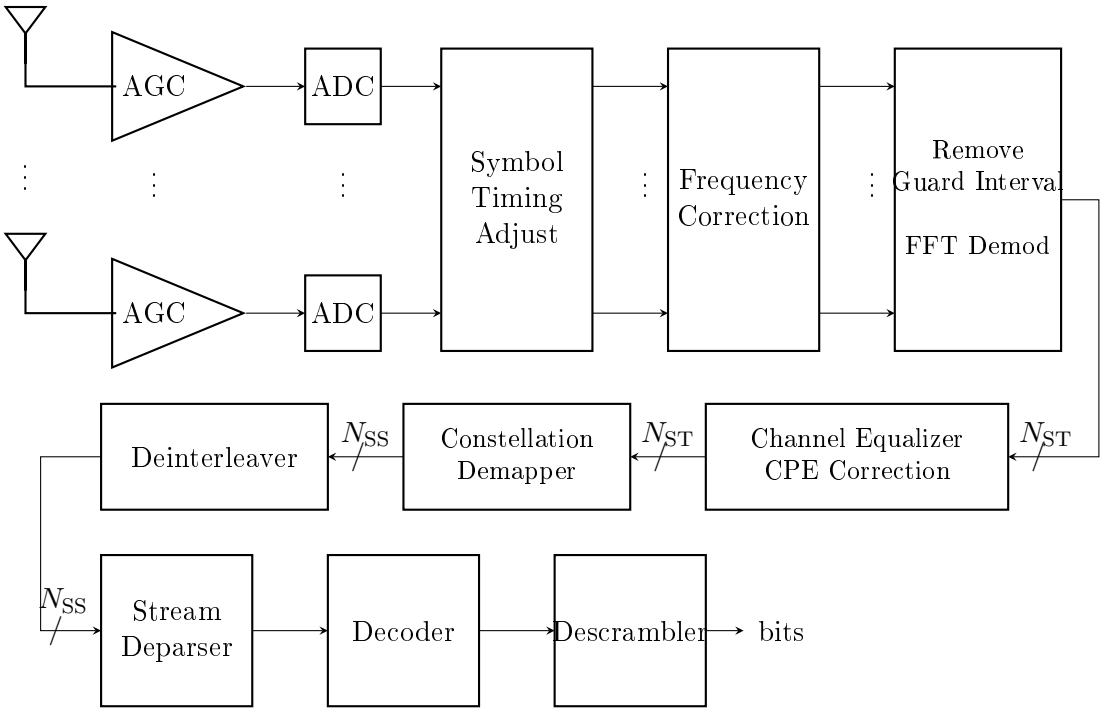

Figure 3.8: Receiver block diagram for MIMO system.

3.3.1 Synchronization

At the side of the receiver, an Analog to Digital Converter (ADC) is used to sample the received signal. The gain is adjusted for an appropriate input signal level using an AGC. The next step is to detect the start of the packet. However 802.11n devices typically have multiple receive antennas, therefore correlation functions for start-of-packet detection and coarse timing should be summed over all the antennas to maximize detection performance.

Packet Detection

Packet detection is the task of finding an approximate estimate of the start of the preamble of an incoming data packet. The simplest algorithm for finding the start edge of the incoming packet is to measure the received signal energy. At every time instant n computed the accumulated energy over some window of length L as follow

$$m_n = \sum_{i=1}^{N_{\mathrm{RX}}} \sum_{k=0}^{L-1} |y_{n-k}^{(i)}|^2 \tag{3.48}$$

When there is no packet, the received signal at the i^{th} antenna consists only of noise $y_n^{(i)} = w_n$. When the packet starts the energy level increased from the signal component $y_n^{(i)} = s_n^{(i)} + w_n$. Thus, the packet can be detected as a change in the received energy level. The main disadvantage of this method is that the received signal strength is unknown and its difficult to set a fixed threshold, which could be used to decide when an incoming packet starts.

Many efficient algorithms for packet detection which exploited the legacy preamble of 802.11 packets are proposed. These detection schemes are based on the repetition of the training symbols in the OFDM signal. The following approach was presented from Schimdl and Cox in [7] for acquiring symbol timing, but the general method is applicable to packet detection. This approach is called the delay and correlate algorithm. It uses two sliding windows C and P where the C window is a crosscorrelation between the received signal and a delayed version of the received signal, and the P window calculates the received signal energy during the crosscorrelation window. The block diagram of the delay and correlate algorithm is shown in Figure 3.9. The delay $D = 16$ is equal to the period of the short training fields. The length L of each window shall be an integer multiple of the delay D.

$$c_n = \sum_{i=1}^{N_{\mathrm{RX}}} \sum_{k=0}^{L-1} y_{n+k}^{(i)} (y_{n+k+D}^{(i)})^* \tag{3.49}$$

$$p_n = \sum_{i=1}^{N_{\mathrm{RX}}} \sum_{k=0}^{L-1} y_{n+k+D}^{(i)} (y_{n+k+D}^{(i)})^* = \sum_{i=1}^{N_{\mathrm{RX}}} \sum_{k=0}^{L-1} |y_{n+k+D}^{(i)}|^2 \tag{3.50}$$

Using the number of the P window to normalize the statistic c_n, we produce the decision statistic m_n which its not dependent on absolute received power level.

$$m_n = \frac{|c_n|^2}{(p_n)^2} \tag{3.51}$$

When the received signal consists of only noise, the output c_n of the delayed crosscorellation is zero mean random variable, since the crosscorrelation of noise samples is zero. Once the start of the packet is received, c_n is a crosscorrelation of the identical short training

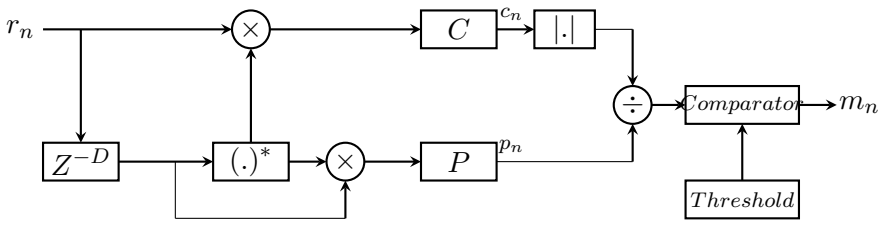

Figure 3.9: Block diagram of delay and correlate algorithm.

symbols, which causes m_n to jump quicly to high values near the one. A threshold value for the statistic m_n is used to be decided the start of the packet. The recommended threshold value is 0.5.

The Delay and Correlate algorithm is used for the packet detection from the WLAN Toolbox. The values of the parameters that used is $D = 16, L = 9*16 = 144$, $m_{thresh} = 0.5$. Packet detected only if the number of correlated peaks is greater than $1.5 \cdot D$ and the relative distance between 1^{st} peak and subsequent peaks is greater than $3 \cdot D$.

Symbol Timing

The packet detection method (coarse symbol timing detection) acquire only rough timing information, and there may still exist a large timing error. After the packet detector has provided an estimate of the start edge of the packet, the symbol timing algorithm(fine symbol timing detection) refines the estimate to sample level precision. The structure of the WLAN packet preamble has the two long training fields for the fine symbol timing detection. The method that we follow for fine symbol timing detection is based in [8] approach. The long training symbol reference sequence is known at the receiver, and it can be correlated with the received noisy signal using a matched filter. Defining the crosscorrelation function

$$\Phi_{ZP}(m) = \sum_{i=1}^{N_{\mathrm{RX}}} \sum_{k=0}^{L-1} y_{m+k}^{(i)} P_k^* \tag{3.52}$$

where L is the length of the preamble and P the known training symbol sequence. A cyclic shift delay is added to the L-LTF for each transmit antenna which causes multiple strong peaks in the correlation function. The multiple peaks affect the accurancy of fine symbol timing estimation. It can be find the location at which its maximum magnitude occurs:

$$\hat{m}_{\max} = \arg\max_{m} |\Phi_{ZP}(m)| \tag{3.53}$$

Another algorithm(that used from MATLAB WLAN Toolbox) selects the earliest sample with magnitude greater than some threshold, usually some percentage of peak magnitude

$$\hat{m}_{TH} = \min\{m \mid |\Phi_{ZP}(m)| > \gamma |\Phi_{ZP}(\hat{m}_{\max})|\}, 0 < \gamma < 1 \tag{3.54}$$

3.3.2 Carrier Frequency Offset (CFO) Estimation

OFDM is a bandwidth efficient signalling scheme for digital communications as in OFDM the spectrum of the individual carriers mutually overlap, giving an optimum spectrum efficiency. The effectiveness of OFDM in the use of spectrum is based on the orthogonality of the subcarriers. One of the principal disadvantages of OFDM is sensitivity to frequency offset in the channel. There are two deleterious effects caused by frequency offset one is the reduction of signal amplitude in the output of the filters matched to each of the subcarriers and the second is introduction of ICI from the other subcarriers [9]. Carrier frequency offset occurs when exists a frequency mismatch in the transmitter and the receiver oscillators. In addition the Doppler shift introduced in the channel causes CFO. Matlab WLAN Toolbox estimates the carrier frequency offset in two stages. At the first stage carriers out the coarse CFO estimation by using the short training symbols, and at the second stage is done the fine CFO estimation by using the long training symbols. The method that uses at the coarse and fine CFO estimation is the same and the estimated frequency offset is given by the equation

$$\Delta f_{\text{est}} = \frac{f_s}{2\pi D} \sum_{i=1}^{N_{\text{RX}}} \sum_{k=n_0}^{n_0+(M-1)D-1} (y_k^{(i)})^* y_{k+D}^{(i)} \tag{3.55}$$

where D is the period(in samples) of the repeated pattern of training symbols that being used, M is the number of training symbols that being used, n_0 is the start each training field, and $y_k^{(i)}$ is the k^{th} value of the received signal in i^{th} antenna. This method is based on the paper [10].

The last two short OFDM symbols are indended by the IEEE 802.11 standardization group for coarse CFO estimation. Yet all of the short OFDM symbols can be used to increase the estimation accuracy. The first short symbol is assuming as a cyclic prefix for the next nine short OFDM symbols. The period of a short OFDM symbol is $D = 16$ and $M = 9$ as the last nine short training symbols is used. For the fine CFO estimation is used the two long OFDM symbols. In this case $D = 64$ and $M = 2$.

3.3.3 Common Phase Error Estimation

The frequency offset will vary during the reception of the packet, making solely initial frequency synchronization insufficient. Furthermore, the system will experience phase noise (PN) invoked by the combination of RF oscillator and the phase-locked loop (PLL). PN causes a common phase turn for all subcarriers, called common phase error (CPE), and a Gaussian-like ICI term. Since the CPE is equal for all subcarriers, it can be estimated and corrected. A way to estimate the common phase noise is to use the pilot signals which are contained in every OFDM symbol. Pilot subcarriers carries known data which altered from the channel and the phase shifts. The rotation of these known pilot symbols, which are observed at the receiver, is a good measure for the CPE. Using the channel estimate

impulse we can calculate an estimation of the received pilots as follows [10]

$$\tilde{s}_{a,i,r} = \sum_{s=1}^{N_{\text{STS}}} P(a,s,i) \cdot \hat{h}_i^{r,s}, \quad i \in \mathcal{P}, 1 \leq r \leq N_{\text{RX}}, 0 \leq a \leq N_{\text{SYM}} - 1, 1 \leq s \leq N_{\text{STS}} \quad (3.56)$$

where P is the reference sequence of pilot signals and h the channel estimation. The common phase noise for the a^{th} symbol given by

$$\theta(a) = \sum_{i \in \mathcal{P}} \sum_{r=1}^{N_{\text{RX}}} \tilde{s}(i,a) s_r^*(i,a) \quad (3.57)$$

where s is the received signal.

Mean Noise Power Estimation

Mean noise power in watts can be estimated using the demodulated pilot symbols in the HT data field and the estimated channel at pilot subcarriers location. Assume that $s \cdot e^{-j\theta(\alpha)}$ denotes the phase correct demodulated pilot signals in the HT data field and the $\tilde{s}$ sequence as defined previously. The pilot error sequence for the r^{th} receive antenna is given by the expression

$$P_r^E(\alpha,i) = \tilde{s}_r(\alpha,i) - s_r(\alpha,i) \cdot e^{-j\theta(\alpha)}, \quad i \in \mathcal{P}, 1 \leq r \leq N_{\text{RX}}, 0 \leq a \leq N_{\text{SYM}} - 1 \quad (3.58)$$

Finally, the noise power estimate is given as follows

$$\hat{N}_0 = \frac{1}{|\mathcal{P}| \cdot N_{\text{RX}}} \sum_{i \in \mathcal{P}} \sum_{r=1}^{N_{\text{RX}}} \Re(P_r^E(i,a) \cdot (P_r^E(i,a))^*) \quad (3.59)$$

The noise power estimation is required if the MMSE equalizer is used.

3.3.4 Channel Estimation

In the HT systems, the receiver uses the HT-LTF field for the MIMO channel estimation.The receiver processes each $3.2\mu s$ long training symbol by removing the cyclic prefix from the HT-LTF and performs an FFT to extract the training subcarriers. The frequency domain representation for each training subcarrier k at the receiver is represented by the equation

$$\mathbf{Y}_{t_i}^k = \begin{bmatrix} y_{1,t_i}^k \\ \vdots \\ y_{N_{\text{RX}},t_i}^k \end{bmatrix} = \begin{bmatrix} h_{1,1}^k & \cdots & h_{1,N_{\text{STS}}}^k \\ \vdots & \ddots & \vdots \\ h_{N_{\text{RX}},1}^k & \cdots & h_{N_{\text{RX}},N_{\text{STS}}}^k \end{bmatrix} \mathbf{p}_{N_{\text{STS}},i} \text{HTLTF}_k + \begin{bmatrix} n_{1,t_i}^k \\ \vdots \\ n_{N_{\text{RX}},t_i}^k \end{bmatrix} \quad (3.60)$$

where t_i is the i^{th} long training symbol, and the symbol n denotes the $AWGN$ terms. The notation $\mathbf{p}_{N_{\text{STS}}}^{(i)}$ denotes the vector that is produced if we take the first N_{STS} elements from

the i^{th} column of matrix $\mathbf{P}$. Furthermore we represented an $N_{\mathrm{SS}} \times N_{\mathrm{LTF}}$ subset of the orthogonal mapping matrix $\mathbf{P}$ with the symbol $\mathbf{P}_{N_{\mathrm{STS}},N_{\mathrm{LTF}}}$.

$$\mathbf{P} = \begin{bmatrix} 1 & -1 & 1 & 1 \\ 1 & 1 & -1 & 1 \\ 1 & 1 & 1 & -1 \\ -1 & 1 & 1 & 1 \end{bmatrix} \tag{3.61}$$

The received signal vector from each time instant(of HT-LTF symbol) is combined into a single matrix, $\begin{bmatrix} \mathbf{Y}^k_{t_1} & \mathbf{Y}^k_{t_2} & \dots & \mathbf{Y}^k_{t_{N_{\mathrm{LTF}}}} \end{bmatrix}$ having the dimensions $N_{RX} \times N_{\mathrm{LTF}}$.

$$\begin{bmatrix} \mathbf{Y}^k_{t_1} & \mathbf{Y}^k_{t_2} & \dots & \mathbf{Y}^k_{t_{N_{\mathrm{LTF}}}} \end{bmatrix} = \begin{bmatrix} h^k_{11} & \dots & h^k_{1N_{\mathrm{STS}}} \\ \vdots & \ddots & \vdots \\ h^k_{N_{\mathrm{RX}}1} & \dots & h^k_{N_{\mathrm{RX}}N_{\mathrm{STS}}} \end{bmatrix} \mathbf{P}_{N_{\mathrm{STS}},N_{\mathrm{LTF}}} \mathrm{HTLTF}_k + \begin{bmatrix} \mathbf{N}^k_{t_1} & \mathbf{N}^k_{t_2} & \dots & \mathbf{N}^k_{t_{N_{\mathrm{LTF}}}} \end{bmatrix} \tag{3.62}$$

To compute the channel estimate matrix we multiply the received signal vector matrix by the transpose of $\mathbf{P}_{N_{STS,N_{\mathrm{LTF}}}}$ and normalize, as follows

$$\begin{bmatrix} \hat{h}^k_{11} & \dots & \hat{h}^k_{1N_{\mathrm{STS}}} \\ \vdots & \ddots & \vdots \\ \hat{h}^k_{N_{\mathrm{RX}}1} & \dots & \hat{h}^k_{N_{\mathrm{RX}}N_{\mathrm{STS}}} \end{bmatrix} = \begin{bmatrix} \mathbf{Y}^k_{t_1} & \mathbf{Y}^k_{t_2} & \dots & \mathbf{Y}^k_{t_{N_{\mathrm{LTF}}}} \end{bmatrix} \mathbf{P}^T_{N_{\mathrm{STS}},N_{\mathrm{LTF}}} \frac{1}{N_{\mathrm{LTF}}\mathrm{HTLTF}_k} \tag{3.63}$$

It's important to note that the channel estimation is done at the start of the packet, thus the channel estimation error will being increasing with the time. If the packet length or the channel varying rate is high, the system performance will decreased.

3.3.5 Channel Equalization

In wireless communications the transmitted signal propagated through a frequency selective environment. By using the OFDM technique a wide band channel is being converted into a set of flat fading channels. In a WLAN receiver it can be used any equalizer for frequency non-selective MIMO channel because for the k^{th} frequency subcarrier, the symbol spaced sequences at input of the equalizer expressed as

$$\mathbf{y}_{k,n} = \mathbf{H}_k \mathbf{x}_{k,n} + \mathbf{n}_{k,n}, \quad 0 \leq n \leq N_{\mathrm{SYM}} \tag{3.64}$$

The equalizer transforms a number of multiplexed received chains N_{RX} into a number of equalized spacial streams N_{SS}. Matlab WLAN Toolbox supports two different equalizers, the Zero Forcing and the Minimum Mean Square equalizer. The Zero Forcing equalizer, it is a linear equalization algorithm that applies an inverse of the frequency response of the the channel to the received signal. The Minimum Mean Square Error equalizer tries to find a matrix $\mathbf{W}$ which minimizes the mean square error $E[||\mathbf{W}\mathbf{y} - \mathbf{x}||_2^2]$. These two equalizers explained furthermore in Section 2.3.3.

3.3.6 Constellation Demapping

The receiver demaps the received equalized symbols $\hat{y}$ using the soft-decision approximate Log Likelihood Ratio (LLR) method for the specified number of coded bits per subcarrier per spatial stream (N_{BPSCS}). It concerns the probability that a bit of a received symbol be 0 or 1, given a set of parameters and possible outcomes. Let us assume that at a particular time instant $\log_2(M) = N_{\text{BPSCS}}$ bits are transmitted in a symbol x, where M represents M-ary signal constellation. Moreover, it is assumed that $c_m(m = 1, 2, \ldots, N_{\text{BPSCS}})$ is the m^{th} coded bit of the transmitted symbol x. Let us also assume that $\mathcal{S} = \{s_1, \ldots, s_M\}$ denotes the set of (complex) constellation symbols. In addition is assumed that each symbol in the constellation is equiprobable ($p(X = s_i) = \frac{1}{M}), \forall\, i = 1, \ldots, M$ where X is a discrete random variable. $\mathcal{S}_0^m$ represents the set of (complex) constellation symbols where the m^{th} bit is 0. Similarly, $\mathcal{S}_1^m$ denotes the set of (complex) constellation symbols where the m^{th} bit is 1. Assuming an AWGN channel per subcarrier and spatial stream after the MMSE or Zero Forcing detector(the output of the MMSE is approximately Gaussian), the signal model can be written as

$$\hat{Y} = \mathbf{W}Y = X + N, \quad N \sim \mathcal{CN}(0, \tilde{N}_0). \tag{3.65}$$

Since the N is a continues Gaussian random value, if $X = s$ where s is a known value, then $\hat{Y} \sim \mathcal{CN}(s, \tilde{N}_0)$. The conditional probability density function (PDF) $f_{\hat{Y}|X=s}(\hat{y})$ is expressed as

$$\begin{aligned} f_{\hat{Y}|X=s}(\hat{y}) &= \frac{1}{\sqrt{2\pi(\tilde{N}_0/2)}} e^{-\frac{|\hat{y}-s|^2}{2(\tilde{N}_0/2)}} \\ &= \frac{1}{\sqrt{\pi\tilde{N}_0}} e^{-\frac{|\hat{y}-s|^2}{\tilde{N}_0}} \end{aligned} \tag{3.66}$$

and from the Bayes rule we have [11],

$$p(X = s|\hat{y}) = \frac{p(X = s) f_{\hat{Y}|X=s}(\hat{y})}{f_{\hat{Y}}(\hat{y})}. \tag{3.67}$$

The definition of LLR for each coded bit can be written as,

$$\begin{aligned} L(c_m) &= \log\left(\frac{p(c_m = 1|y)}{p(c_m = 0|y)}\right) \\ &= \log\left(\frac{p(c_m = 1|\hat{y})}{p(c_m = 0|\hat{y})}\right) \\ &= \log\left(\frac{\sum_{s\in\mathcal{S}_1^m} p(s|\hat{y})}{\sum_{s\in\mathcal{S}_0^m} p(s|\hat{y})}\right). \end{aligned} \tag{3.68}$$

Using the Equation (3.67),

$$\begin{aligned} L(c_m) &= \log\left(\frac{\sum_{s\in\mathcal{S}_1^m} f_{\hat{Y}|X=s}(\hat{y})p(X=s)}{\sum_{s\in\mathcal{S}_0^m} f_{\hat{Y}|X=s}(\hat{y})p(X=s)}\right) \\ &\overset{p(X=s)=1/M}{=} \log\left(\frac{\sum_{s\in\mathcal{S}_1^m} f_{\hat{Y}|X=s}(\hat{y})}{\sum_{s\in\mathcal{S}_0^m} f_{\hat{Y}|X=s}(\hat{y})}\right) \end{aligned} \tag{3.69}$$

where $f_{\hat{Y}|X=s}(\hat{y})$ is the conditional PDF of the MMSE output and $p(X=s)$ is the probability of a symbol in a signal constellation. Thus, using the equations 3.66 and (3.69) the LLR value of the c_m is given by

$$L(c_m) = \log\left(\frac{\sum_{s\in\mathcal{S}_1^m} e^{-\frac{|\hat{y}-s|^2}{\tilde{N}_0}}}{\sum_{s\in\mathcal{S}_0^m} e^{-\frac{|\hat{y}-s|^2}{\tilde{N}_0}}}\right). \tag{3.70}$$

This demapper which calculates an LLR is known as LogAPP (logarithmic a-posteriori probability or LogMAP) demmaper [12]. Also is known as Exact LLR. Due to the complicated mathematical operations of LogAPP algorithm the max-log approximation LLR algorithm is used. The MaxLog demapper is an algorithm that calculates LLR by using only the two closest constellation points with the bit value at the given bit position. The log-sum exponential approximation [13] is

$$\log\left(\sum_i e^{\phi_i}\right) \approx \max_i(\phi_i). \tag{3.71}$$

Combining the equations (3.71) and (3.70), we have

$$\begin{aligned} L(c_m) &\approx \log\left(\frac{\exp\left(\max\limits_{s\in\mathcal{S}_1^m}\left\{-\frac{|\hat{y}-s|^2}{\tilde{N}_0}\right\}\right)}{\exp\left(\max\limits_{s\in\mathcal{S}_1^m}\left\{-\frac{|\hat{y}-s|^2}{\tilde{N}_0}\right\}\right)}\right) \\ &= \frac{1}{\tilde{N}_0}\left(\min_{s\in\mathcal{S}_0^m}\{|\hat{y}-s|^2\} - \min_{s\in\mathcal{S}_1^m}\{|\hat{y}-s|^2\}\right). \end{aligned} \tag{3.72}$$

The result is a value indicating whether that bit is more likely to be a one or zero. For each input symbol to constellation demapper the output is N_{BPSCS} real numbers.

3.3.7 Deinterleaver & Decoder

The length of the output N_{SS} streams of constellation demapper is $N_{\mathrm{SD}} \cdot N_{\mathrm{BPSCS}}(i_{\mathrm{SS}}) \cdot N_{\mathrm{SYM}} = N_{\mathrm{CBPSS}}(i_{\mathrm{SS}})$. These streams deinterleaved separately by the deinterleaver which

inverses the three permutations that performed to interleaver. The inverse of third permutation is

$$j = \left(r + \left((2(i_{\mathrm{SS}} - 1)) \bmod 3 + 3 \cdot \left\lfloor \frac{i_{\mathrm{SS}} - 1}{3} \right\rfloor \right) \cdot N_{\mathrm{ROT}} \cdot N_{\mathrm{BPSCS}}(i_{\mathrm{SS}}) \right) \bmod N_{\mathrm{CBPSS}}(i_{\mathrm{SS}}), \quad r = 0, 1, \ldots, N_{\mathrm{CBPSS}}(i_{\mathrm{SS}}) - 1 \tag{3.73}$$

The inverse of second permutation is

$$i = s(i_{\mathrm{SS}}) \cdot \left\lfloor \frac{j}{s(i_{\mathrm{SS}})} \right\rfloor + \left(j + \left\lfloor N_{\mathrm{COL}} \frac{j}{N_{\mathrm{CBPSS}}(i_{\mathrm{SS}})} \right\rfloor \right) \bmod s(i_{\mathrm{SS}}), \quad j = 0, 1, \ldots, N_{\mathrm{CBPSS}}(i_{\mathrm{SS}}) - 1 \tag{3.74}$$

The inverse of first permutation is

$$k = N_{\mathrm{COL}} \cdot i - (N_{\mathrm{CBPSS}}(i_{\mathrm{SS}}) - 1) \cdot \left\lfloor \frac{i}{N_{\mathrm{ROW}}} \right\rfloor, \quad i = 0, 1, \ldots, N_{\mathrm{CBPSS}}(i_{\mathrm{SS}}) - 1 \tag{3.75}$$

Assuming that $\mathbf{z}^i$ denotes the output of the constellation demapper of i^{th} spatial stream, the r^{th} symbol of the stream is reordered from the deinterleaver in the k^{th} index as shown in Figure 3.10.

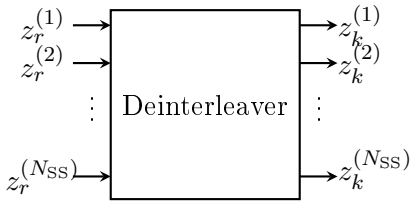

Figure 3.10: Deinterleaver scheme.

As the final step in the deinterleaving process, the stream parsing operation is reversed by taking blocks of s bits from each spatial stream in a round robin fashion to create a single bit stream for the decoder. The single bit stream is decoded using the Viterbi decoder, as recomended from the IEEE. Finally the output stream of decoder is descrambled. The descrambler structure is same as scrambler structure in Figure 3.6.

Chapter 4

HT MIMO OFDM Systems Analysis

4.1 Introduction

In this chapter we will analyze some HT OFDM systems with different MIMO schemes and define three SNR values in different stages of the receiver. On the receiver side of OFDM systems, after the FFT demodulation process, N_{ST} channels are processed in parallel as the channel gain of each subcarrier is varying and the Signal to Noise Ratio (SNR) is different in each subcarrier. The number of errors in the bit streams which are transmitted through a channel increases with the decrease of the SNR value of the subcarrier. As a result, system performance depends immediately from the channel gain of each subcarrier.

As it has been described the indices of pilot subcarriers in HT OFDM system are scattered on the range of data subcarrier indices which are placed around the DC. To simplify the mathematical expressions, we assume that we remapping the indices by using the mapping function

$$I(k) = \begin{cases} \mathbf{I}_{\mathrm{data},k} & 1 \leq k \leq N_{\mathrm{SD}}, \\ \mathbf{I}_{\mathrm{pilot},k} & N_{\mathrm{SD}}+1 \leq k \leq N_{\mathrm{ST}} \end{cases} \tag{4.1}$$

where the vector $\mathbf{I}_{\mathrm{data}}$ contains the data subcarrier indices and the $\mathbf{I}_{\mathrm{pilot}}$ vector, the pilot subcarrier indices respectively. The notation $\mathbf{I}_{\mathrm{data},k}$ represents the k^{th} element of the vector. Therefore, in the rest of this report we assume that the data subcarrier indices are in the range $1 \leq k \leq N_{\mathrm{SD}}$ and the pilot subcarrier indices in the range $N_{\mathrm{SD}}+1 \leq k \leq N_{\mathrm{ST}}$.

Post-Processing SNR Definition

In the effort to extract a single SNR value from the various SNRs per subcarrier we define the post-processing SNR γ_{aver} as presented in Figure 4.2. More specifically, the N parallel data streams are grouped in a sequence on which is calculated the signal to noise ratio. The process to compute the mean power of a sequence $\mathbf{s}$ which is constructed from M streams is shown in Figure 4.1.

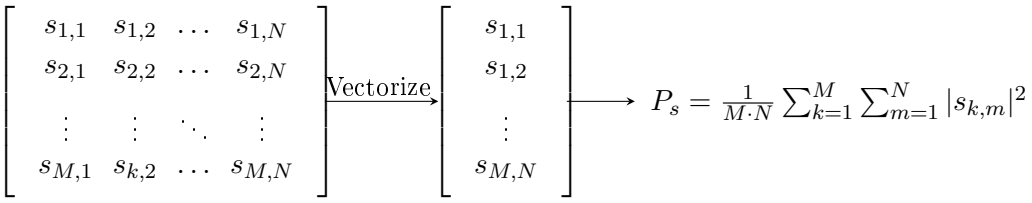

Figure 4.1: Calculation of the mean power over M parallel streams with N time instances.

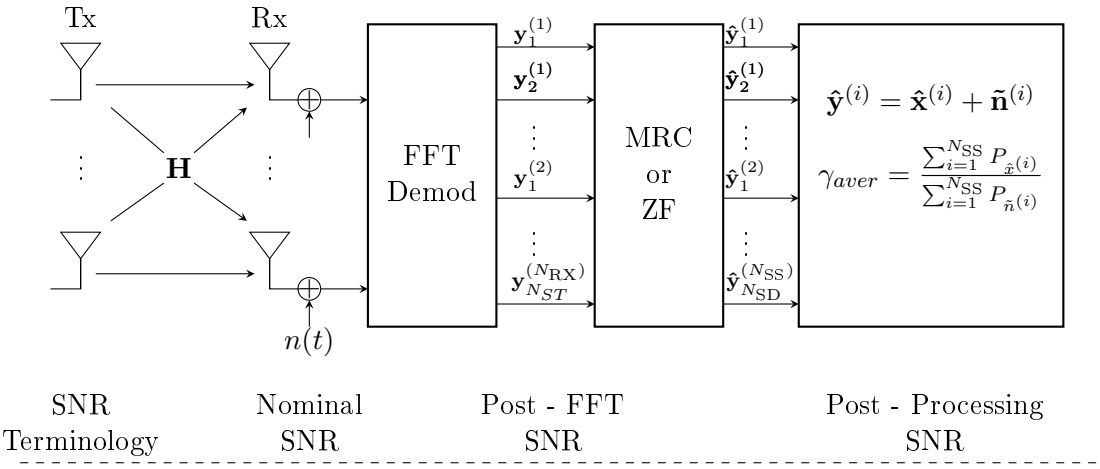

Figure 4.2: A block diagram of a part of the receiver structure and description of SNR terminologies.

4.2 SISO OFDM System

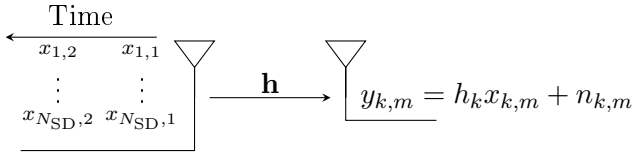

Figure 4.3: SISO OFDM system

Let us assume a SISO OFDM system which transmits the stream of constellation points x. This stream is divided into N_{SYM} groups of length N_{SD} which constitute the OFDM

symbols. The sequences of OFDM symbols can be represented by the matrix $\mathbf{X}$ as defined in Equation (4.2)

$$\mathbf{X} = \begin{bmatrix} x_{1,1} & x_{1,2} & \cdots & x_{1,N_{\mathrm{SYM}}} \\ x_{2,1} & x_{2,2} & \cdots & x_{2,N_{\mathrm{SYM}}} \\ \vdots & \vdots & \ddots & \vdots \\ x_{N_{\mathrm{SD}},1} & x_{N_{\mathrm{SD}},2} & \cdots & x_{N_{\mathrm{SD}},N_{\mathrm{SYM}}} \end{bmatrix} \tag{4.2}$$

where $x_{k,m}$ denotes the symbols which transmitted at the m^{th} OFDM symbol, and at the k^{th} subcarrier. The mean power of the constellation points denoted with σ_x^2 is equal to one. The received signal $y(t)$ in the continuous time domain is the product of the convolution between the transmitted signal $x(t)$ and the channel response $h(t)$ plus the thermal noise which caused from the receiver electronics.

$$y(t) = x(t) * h(t) + n(t) \tag{4.3}$$

Assuming that the receiver is perfect synchronized and the received signal has demodulated by the FFT transformation, the symbol spaced sequences in the frequency domain can be represented by the matrix $\mathbf{Y}$ respectively to the matrix $\mathbf{X}$.

$$\mathbf{Y} = \begin{bmatrix} y_{1,1} & y_{1,2} & \cdots & y_{1,N_{\mathrm{SYM}}} \\ y_{2,1} & y_{2,2} & \cdots & y_{2,N_{\mathrm{SYM}}} \\ \vdots & \vdots & \ddots & \vdots \\ y_{N_{\mathrm{SD}},1} & y_{N_{\mathrm{SD}},2} & \cdots & y_{N_{\mathrm{SD}},N_{\mathrm{SYM}}} \end{bmatrix} \tag{4.4}$$

The SNR definition at the input of the receiver is

$$\mathrm{SNR}_0 = \frac{\varepsilon\{|x(t) * h(t)|^2\}}{N_0} \tag{4.5}$$

where N_0 is the noise variance. As it has been described(in section 2.2.3) some of the subcarriers are nulled and only the N_{ST} subcarriers are carrying data(information symbols or pilots). After the FFT process at the receiver, the noise terms which corresponds in unused subcarriers are discarded and the SNR increases. Defining in the frequency domain the channel vector

$$\mathbf{h} = \begin{bmatrix} h_1 \\ h_2 \\ \vdots \\ h_{N_{\mathrm{SD}}} \end{bmatrix}, \tag{4.6}$$

each received symbol $y_{k,m}$ can be expressed as

$$y_{k,m} = h_k \cdot x_{k,m} + \hat{n}_{k,m}, \quad \hat{n}_{k,m} \sim \mathcal{CN}(0, \hat{N}_0) \tag{4.7}$$

where $\hat{N}_0 = (N_{\mathrm{ST}}/N_{\mathrm{FFT}})N_0$. Thus, the SNR value after the FFT process is given by the following equation

$$\begin{aligned}\mathrm{SNR}_1 &= \frac{\sum_{k=1}^{N_{\mathrm{ST}}}\sum_{m=1}^{N_{\mathrm{SYM}}}|h_k \cdot x_{k,m}|^2}{\sum_{k=1}^{N_{\mathrm{ST}}}\sum_{m=1}^{N_{\mathrm{SYM}}}|\hat{n}_{k,m}|^2} \\ &= \sum_{k=1}^{N_{\mathrm{ST}}}\frac{|h_k|^2\sigma_x^2}{N_{\mathrm{ST}}\hat{N}_0} = \frac{N_{\mathrm{FFT}}}{N_{\mathrm{ST}}}\sum_{k=1}^{N_{\mathrm{ST}}}\frac{|h_k|^2\sigma_x^2}{N_0}.\end{aligned} \tag{4.8}$$

Since the FFT process doesn't change the mean power of a signal, we can conclude that

$$\mathrm{SNR}_0 = \frac{N_{\mathrm{ST}}}{N_{\mathrm{FFT}}}\mathrm{SNR}_1 = \sum_{k=1}^{N_{\mathrm{ST}}}\frac{|h_k|^2\sigma_x^2}{N_{\mathrm{ST}}N_0}. \tag{4.9}$$

Defining the channel estimate vector $\hat{\mathbf{h}}$ accordingly to the $\mathbf{h}$, and performing the maximum ratio combining detector, is produced the matrix

$$\hat{\mathbf{Y}} = \begin{bmatrix} \hat{y}_{1,1} & \hat{y}_{1,2} & \cdots & \hat{y}_{1,N_{\mathrm{SYM}}} \\ \hat{y}_{2,1} & \hat{y}_{2,2} & \cdots & \hat{y}_{2,N_{\mathrm{SYM}}} \\ \vdots & \vdots & \ddots & \vdots \\ \hat{y}_{N_{\mathrm{SD}},1} & \hat{y}_{N_{\mathrm{SD}},2} & \cdots & \hat{y}_{N_{\mathrm{SD}},N_{\mathrm{SYM}}} \end{bmatrix}. \tag{4.10}$$

If we make the assumption that $\hat{h}_k \approx h_k$, the equalized symbols are

$$\hat{y}_{k,m} = \frac{\hat{h}_k^* h_k}{|\hat{h}_k|^2}x_{k,m} + \frac{\hat{h}_k^*}{|\hat{h}_k|^2}\hat{n}_{k,m} = x_{k,m} + \tilde{n}_{k,m}, \quad \tilde{n}_{k,m} \sim \mathcal{CN}(0, (1/|h_k|^2) \cdot \hat{N}_0) \tag{4.11}$$

and the SNR of the k^{th} subcarrier is

$$\gamma_k = \frac{|h_k|^2\sigma_x^2}{\hat{N}_0}. \tag{4.12}$$

The post-processing SNR can be expressed as

$$\begin{aligned}\gamma_{aver} &= \frac{\sum_{k=1}^{N_{\mathrm{SD}}}\sum_{m=1}^{N_{\mathrm{SYM}}}|x_{k,m}|^2}{\sum_{k=1}^{N_{\mathrm{SD}}}\frac{1}{|h_k|^2}\sum_{m=1}^{N_{\mathrm{SYM}}}|\hat{n}_{k,m}|^2} \\ &= \frac{N_{\mathrm{SD}} \cdot \sigma_x^2}{\sum_{k=1}^{N_{\mathrm{SD}}}\frac{1}{|h_k|^2}\hat{N}_0}.\end{aligned} \tag{4.13}$$

Since the pilot subcarrier indices are scattered in the whole bandwidth, and the channel responses for adjacent subcarriers tends to be equal, an approximation of the SNR_1 is

$$\mathrm{SNR}_1 = \sum_{k=1}^{N_{\mathrm{ST}}}\frac{|h_k|^2\sigma_x^2}{N_{\mathrm{ST}}\hat{N}_0} \approx \sum_{k=1}^{N_{\mathrm{SD}}}\frac{|h_k|^2\sigma_x^2}{N_{\mathrm{SD}}\hat{N}_0}. \tag{4.14}$$

Therefore, combining the equations (4.14) and (4.13)

$$\begin{aligned}\gamma_{aver} &= \frac{N_{\mathrm{SD}} \cdot \sigma_x^2 \sum_{k=1}^{N_{\mathrm{SD}}} |h_k|^2}{\sum_{k=1}^{N_{\mathrm{SD}}} \frac{1}{|h_k|^2} \sum_{k=1}^{N_{\mathrm{SD}}} |h_k|^2 \hat{N}_0} \\ &\approx \frac{N_{\mathrm{SD}}^2 \cdot \mathrm{SNR}_1}{\sum_{k=1}^{N_{\mathrm{SD}}} \frac{1}{|h_k|^2} \sum_{k=1}^{N_{\mathrm{SD}}} |h_k|^2} \\ &= \frac{N_{\mathrm{SD}}^2}{\sum_{k=1}^{N_{\mathrm{SD}}} \frac{1}{|h_k|^2} \sum_{k=1}^{N_{\mathrm{SD}}} |h_k|^2} \cdot \frac{N_{\mathrm{FFT}}}{N_{\mathrm{ST}}} \cdot \mathrm{SNR}_0\end{aligned} \tag{4.15}$$

4.3 SIMO OFDM System

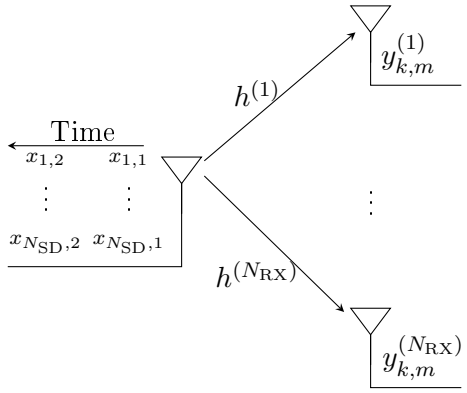

Figure 4.4: Receive diversity scheme.

To achieve higher performance of the system, without increasing the transmit power, multiple antennas at the receiver can be used. We define the matrix $\mathbf{X}$ similarly with the previous section and the received symbol spaced sequence at the k^{th} subcarrier and the i^{th} receive antenna is

$$y_{k,m}^{(i)} = h_k^{(i)} x_{k,m} + \hat{n}_{k,m}^{(i)}, \quad \hat{n}_{k,m}^{(i)} \sim \mathcal{CN}(0, \hat{N}_0). \tag{4.16}$$

Assuming that all the antennas are identical, and the noise variance in each of them is N_0, the SNR value at the input of the receiver is

$$\mathrm{SNR}_0 = \sum_{i=1}^{N_{\mathrm{RX}}} \frac{\varepsilon\{|x(t) * h^{(i)}(t)|^2\}}{\varepsilon\{|n^{(i)}(t)|^2\}} = \sum_{k=1}^{N_{\mathrm{ST}}} \frac{||\mathbf{h}_k||_2^2 \sigma_x^2}{N_{\mathrm{ST}} \cdot N_0} \tag{4.17}$$

where $\mathbf{h}_k = [h_k^{(1)} \ \ldots \ h_k^{(N_{\mathrm{RX}})}]^T$. Also the SNR value after the FFT process is $\mathrm{SNR}_1 = (N_{\mathrm{FFT}}/N_{\mathrm{ST}})\mathrm{SNR}_0$. As has explained in the section 2.3.1 the MRC output for the k^{th}

subcarrier expressed as

$$\begin{aligned}\hat{y}_{k,m} &= x_{k,m} + \frac{\mathbf{h}_k^H}{||\mathbf{h}_k||_2^2}\hat{\mathbf{n}}_{k,m} \\ &= x_{k,m} + \tilde{n}_{k,m}, \quad \tilde{n}_{k,m} \sim \mathcal{CN}(0, (1/||\mathbf{h}_k||_2^2) \cdot \hat{N}_0)\end{aligned} \tag{4.18}$$

The SNR of the k^{th} subcarrier is given by the expression

$$\begin{aligned}\hat{\gamma_k} &= \frac{\varepsilon\{x_{k,m}^* x_{k,m}\}}{\frac{1}{||\mathbf{h}_k||^4}\varepsilon\{|h_k^{(1)}\hat{n}_{k,m}^{(1)}|^2 + \cdots + |h_k^{(N_{\mathrm{RX}})}\hat{n}_{k,m}^{(N_{\mathrm{RX}})}|^2\}} \\ &= \frac{||\mathbf{h}_k||^4\sigma_x^2}{|h_k^{(1)}|^2\varepsilon\{|\hat{n}_{k,m}^{(1)}|^2\} + \cdots + |h_k^{(N_{\mathrm{RX}})}|^2\varepsilon\{|\hat{n}_{k,m}^{(N_{\mathrm{RX}})}|^2\}} \\ &= \frac{||\mathbf{h}_k||^2\sigma_x^2}{\hat{N}_0}.\end{aligned} \tag{4.19}$$

At the Equation (4.19) is used that $\varepsilon\{n_{k,m}^{(i)} n_{k,m}^{(j)}\} = 0$ when $i \neq j$ since the noise terms are uncorrelated, and then the mean of the sum is splitted into a sum of means since the noise terms are independent. The post-processing SNR is calculated as follows(similar with the Equation (4.15))

$$\gamma_{\mathrm{aver}} = \frac{N_{\mathrm{SD}}^2}{\sum_{k=1}^{N_{\mathrm{SD}}} \frac{1}{||\mathbf{h}_k||^2} \sum_{k=1}^{N_{\mathrm{SD}}} ||\mathbf{h}_k||^2} \cdot \frac{N_{\mathrm{FFT}}}{N_{\mathrm{ST}}} \cdot \mathrm{SNR}_0 \tag{4.20}$$

4.4 MISO OFDM System

An another way to to achieve higher diversity order is to use multiple antennas at the transmitter. Assuming that the channel response is known at the transmitter, we performing the transmit beamforming technique and the transmitted symbols at the k^{th} subcarrier and the m^{th} time slot are given by the equation:

$$\tilde{\mathbf{x}}_{k,m} = \frac{\mathbf{h}_k^*}{||\mathbf{h}_k||_2} x_{k,m}, \quad 0 \leq m \leq N_{\mathrm{SYM}} - 1 \tag{4.21}$$

Note that the total transmitted power over all transmit antennas is equal to $\varepsilon\{\tilde{x}_{k,m}^* \tilde{x}_{k,m}\} = \sigma_x^2$.

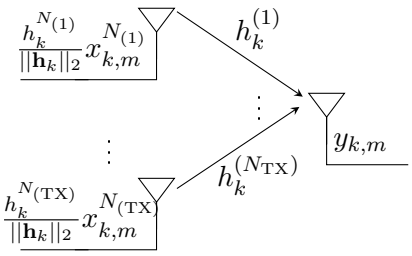

Figure 4.5: Transmit Beamforming technique

The received symbol spaced stream expressed as

$$y_{k,m} = \mathbf{h}_k^T \frac{\mathbf{h}_k^*}{||\mathbf{h}_k||_2} x_{k,m} + \hat{n}_{k,m}, \quad n \sim \mathcal{CN}(0, \hat{N}_0) \tag{4.22}$$

The SNRs per subcarrier are:

$$\gamma_k = \frac{||\mathbf{h}_k||_2^2 \varepsilon\{x_{k,m}^* x_{k,m}\}}{\varepsilon\{\hat{n}_{k,m}^* \hat{n}_{k,m}\}} = \frac{||\mathbf{h}_k||_2^2 \sigma_x^2}{\hat{N}_0}, \quad 1 \le k \le N_{\mathrm{SD}} \tag{4.23}$$

In this specific case, the estimated channel vector is not approximately equal with the true channel response because the transmitted symbols are beamformed with the channel response. As a result, the channel estimate vector is $\hat{\mathbf{h}}_k = ||\mathbf{h}_k||_2$ and the equalized symbol sequences per subcarrier are

$$\hat{y}_{k,m} = x_{k,m} + \frac{1}{||\mathbf{h}_k||_2} \hat{n}_{k,m}. \tag{4.24}$$

The SNR_0 value at the input of the receiver and the SNR_1 value post the FFT demodulation are

$$\mathrm{SNR}_0 = \frac{\sum_{k=1}^{N_{\mathrm{ST}}} ||\mathbf{h}_k||_2^2}{N_{\mathrm{ST}} N_0}, \quad \mathrm{SNR}_1 = \frac{N_{\mathrm{FFT}}}{N_{\mathrm{ST}}} \mathrm{SNR}_0 \tag{4.25}$$

Finally, the post processing SNR value at the input of the decoder is

$$\gamma_{\mathrm{aver}} = \frac{N_{SD}^2}{\sum_{k=1}^{N_{\mathrm{SD}}} \frac{1}{||\mathbf{h}_k||^2} \sum_{k=1}^{N_{\mathrm{SD}}} ||\mathbf{h}_k||^2} \cdot \frac{N_{\mathrm{FFT}}}{N_{\mathrm{ST}}} \cdot \mathrm{SNR}_0 \tag{4.26}$$

4.5 MIMO OFDM System

Alamouti STBC

For Alamouti STBC modes in the general case with $N_{\mathrm{TX}} = 2$ transmit antennas, and N_{RX} receive antennas, at two time slots are being transmitted two symbols as is shown in Figure 4.6.

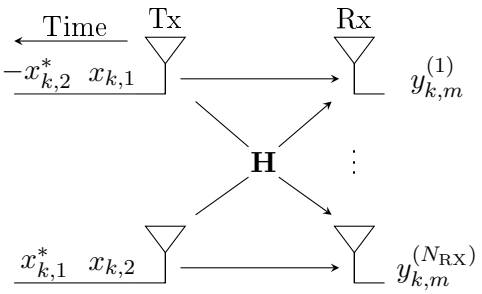

Figure 4.6: Alamouti Coding Scheme.

The sequence of the complex symbols which encodes the data, divided into two matrices. The first matrix represents the transmitted data symbols in the frequency domain from the first antenna.

$$\mathbf{X}^{(1)} = \begin{bmatrix} x_{1,1} & -x^*_{1,2} & \cdots & x_{1,N_{\mathrm{SYM}}-1} & -x^*_{1,N_{\mathrm{SYM}}} \\ x_{2,1} & -x^*_{2,2} & \cdots & x_{2,N_{\mathrm{SYM}}-1} & -x^*_{2,N_{\mathrm{SYM}}} \\ \vdots & \vdots & \ddots & \vdots & \vdots \\ x_{N_{\mathrm{SD}},1} & -x^*_{N_{\mathrm{SD}},2} & \cdots & x_{N_{\mathrm{SD}},N_{\mathrm{SYM}}-1} & -x^*_{N_{\mathrm{SD}},N_{\mathrm{SYM}}} \end{bmatrix} \tag{4.27}$$

Respectively, table $\mathbf{X}^{(2)}$ contains the symbols transmitted by the second antenna of the transmitter.

$$\mathbf{X}^{(2)} = \begin{bmatrix} x_{1,2} & x^*_{1,1} & \cdots & x_{1,N_{\mathrm{SYM}}} & x^*_{1,N_{\mathrm{SYM}}-1} \\ x_{2,2} & x^*_{2,1} & \cdots & x_{2,N_{\mathrm{SYM}}} & x^*_{2,N_{\mathrm{SYM}}-1} \\ \vdots & \vdots & \ddots & \vdots & \vdots \\ x_{N_{\mathrm{SD}},2} & x^*_{N_{\mathrm{SD}},1} & \cdots & x_{N_{\mathrm{SD}},N_{\mathrm{SYM}}} & x^*_{N_{\mathrm{SD}},N_{\mathrm{SYM}}-1} \end{bmatrix} \tag{4.28}$$

The transmit power σ_x^2 is uniformly distributed over the transmit antennas such that the signal variance per antenna is σ_x^2/N_{TX}, and the SNR at the input of the receiver is given by the equation:

$$\mathrm{SNR}_0 = \sum_{i=1}^{N_{\mathrm{RX}}} \sum_{k=1}^{N_{\mathrm{ST}}} \frac{(|h_{k,i1}|^2 + |h_{k,i2}|^2)\sigma_x^2}{2 \cdot N_{\mathrm{ST}} \cdot N_0}. \tag{4.29}$$

where $h_{k,ij}$ denotes the channel coefficient from Tx antenna j to Rx antenna i, of the k^{th} subcarrier. Hence, the channel matrix per subcarrier expressed as

$$\mathbf{H}_k = \begin{bmatrix} \mathbf{h}_{k,1} & \mathbf{h}_{k,2} \end{bmatrix} = \begin{bmatrix} h_{k,11} & h_{k,12} \\ h_{k,21} & h_{k,22} \\ \vdots & \vdots \\ h_{k,N_{\mathrm{RX}},1} & h_{k,N_{\mathrm{RX}},2} \end{bmatrix}. \tag{4.30}$$

The vector $\mathbf{h}_k$ is defined to contain all the elements of the matrix $\mathbf{H}_k$. After the STBC combine processing as explained in section 2.3.2 the statistics for the two symbols which transmitted simultaneously at two time slots, at the k^{th} subcarrier are:

$$\hat{y}_{k,m} = x_{k,m} + \tilde{n}_{k,m}, \quad \tilde{n}_{k,m} \sim \mathcal{CN}\left(0, \left(\frac{1}{||\mathbf{h}_k||_2^2}\right)\hat{N}_0\right) \tag{4.31}$$

$$\hat{y}_{k,m+1} = x_{k,m+1} + \tilde{n}_{k,m+1}, \quad \tilde{n}_{k,m+1} \sim \mathcal{CN}\left(0, \left(\frac{1}{||\mathbf{h}_k||_2^2}\right)\hat{N}_0\right) \tag{4.32}$$

The SNR of each subcarrier is [14]

$$\gamma_k = \frac{(||\mathbf{h}_k||_2^2)\cdot\sigma_x^2}{N_{TX}\cdot N_0}, \quad 1 \le k \le N_{\mathrm{SD}} \tag{4.33}$$

and the post-processing SNR it can be computed by the form

$$\gamma_{\mathrm{aver}} = \frac{N_{\mathrm{SD}}^2}{\sum_{k=1}^{N_{\mathrm{SD}}} ||\mathbf{h}_k||_2^2 \sum_{k=1}^{N_{\mathrm{SD}}} \frac{1}{||\mathbf{h}_k||_2^2}} \frac{N_{\mathrm{FFT}}}{N_{\mathrm{ST}}} \mathrm{SNR}_0. \tag{4.34}$$

Spatial Multiplexing

The 802.11n standard supports MIMO systems up to 4×4 schemes. When the channel state is "good", multiple spatial streams can be used, increasing the data rate linearly with the number of spatial streams. Assuming a 2×2 MIMO system with 2 spatial streams the information symbols are separated into the spatial streams, constructing the matrices $\mathbf{X}^{(i)}, i = 1, 2$. The system is shown in Figure 4.7.

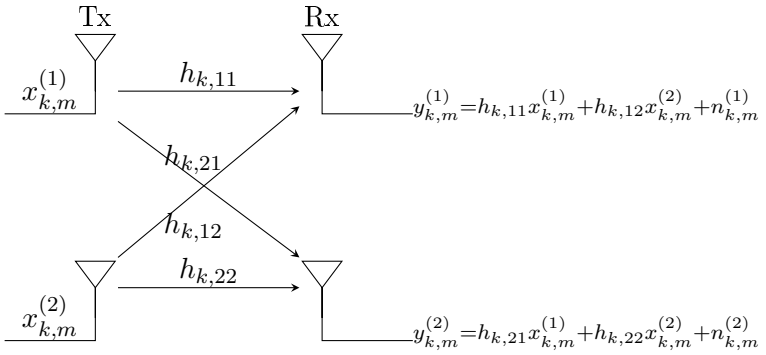

Figure 4.7: 2×2 MIMO system.

We define the channel matrix per subcarrier

$$\mathbf{H}_k = \begin{bmatrix} h_{k,11} & h_{k,12} \\ h_{k,21} & h_{k,22} \end{bmatrix} \tag{4.35}$$

where $h_{k,ij}$ is the complex channel parameter between i^{th} receive and j^{th} transmitte for the k^{th} subcarrier. In addition, we define the parameters $H_{i,k}^2 = \sum_{q=1}^{2} |h_{k,qi}|^2, i = 1, 2$ which will be used to simplify mathematical expressions. The nominal SNR is given by the equation

$$\mathrm{SNR}_0 = \sum_{k=1}^{N_{\mathrm{ST}}} \frac{H_{1,k}^2 + H_{2,k}^2}{N_{\mathrm{ST}} N_0} \tag{4.36}$$

The received symbols at k^{th} subcarrier index are shown below

$$\mathbf{y}_{k,m} = \begin{bmatrix} y_{k,m}^{(1)} \\ y_{k,m}^{(2)} \end{bmatrix} = \begin{bmatrix} h_{k,11} & h_{k,12} \\ h_{k,21} & h_{k,22} \end{bmatrix} \begin{bmatrix} x_{k,m}^{(1)} \\ x_{k,m}^{(2)} \end{bmatrix} + \begin{bmatrix} \hat{n}_{k,m}^{(1)} \\ \hat{n}_{k,m}^{(2)} \end{bmatrix} \tag{4.37}$$

Using the Zero Forcing detector the equalized symbols are given by the equation:

$$\hat{\mathbf{y}}_{k,m} = \begin{bmatrix} \hat{y}_{k,m}^{(1)} \\ \hat{y}_{k,m}^{(2)} \end{bmatrix} = \begin{bmatrix} x_{k,m}^{(1)} \\ x_{k,m}^{(2)} \end{bmatrix} + \begin{bmatrix} \tilde{n}_{k,m}^{(1)} \\ \tilde{n}_{k,m}^{(2)} \end{bmatrix} \tag{4.38}$$

where $\tilde{n}_{k,m}^{(i)} \sim \mathcal{CN}(0, H_{i,k}^2 / det\left(\mathbf{H}_k \cdot \mathbf{H}_k^H\right) \hat{N}_0)$. The SNRs per subcarrier and spatial stream are

$$\gamma_{k,1} = \frac{\sigma_x^2 \cdot |\det(\mathbf{H}_k)|^2}{\hat{N}_0 H_{1,k}^2} \tag{4.39}$$

$$\gamma_{k,2} = \frac{\sigma_x^2 \cdot |\det(\mathbf{H}_k)|^2}{\hat{N}_0 H_{2,k}^2} \tag{4.40}$$

Note that $|det(\mathbf{H}_k)|^2 = det(\mathbf{H}_k \cdot \mathbf{H}_k^H)$. The post-processing SNR expressed as

$$\gamma_{\mathrm{aver}} = \frac{2 \cdot N_{\mathrm{SD}}}{\sum_{k=1}^{N_{\mathrm{SD}}} \frac{||\mathbf{h}_k||_2^4}{|\det(\mathbf{H}_k)|^2}} \frac{N_{\mathrm{FFT}}}{N_{\mathrm{ST}}} \mathrm{SNR}_0 \tag{4.41}$$

where $\mathbf{h}_k$ is the vectorized matrix $\mathbf{H}_k$.

Chapter 5

Exponential Effective SNR Mapping

5.1 Introdution

The modern wireless communication systems are designed to provide high data rate. The basic ways to increase the data rate are larger channel bandwidth with utilization of a higher number of data subcarriers, larger size of constellation, higher coding rate and use of multiple antennas. In addition, a method to increase the performance without extend the channel bandwidth is is the adaptive modulation and coding (AMC). In AMC, the transmitter selects its modulation coding scheme out of a limited set of MCSs with respect to the channel conditions to increase the throughput, controlled by a restriction on the probability of error. WLAN standards 802.11n , 802.11ac , 802.11ad, defines a protocol that allows to adjust the modulation and coding scheme according to current channel condition in order to increase throughput. The link adaptation algorithms which used to select the MCS, are must predict the BER(or PER) in small time duration. As result of the frequency selective characteristics of the wideband channel, the channel gains of these subcarriers can be completely different. Consequently, the right MCS needs to be determined as a function of a vector of subcarrier gains. Link Quality Metrics (LQMs) have been recommended to make easier this issue and allow it to be comparable to AMC through narrowband channels. An LQM maps the vector of signal to noise ratios to a scalar, which is then quickly mapped to BER(or PER) using a 1- dimensional look-up-table.

To evaluate the system performance by means of classical link simulations, where transmission at the symbol level is modeled, with detailed channel modeling it may have large complexity. To obtain a good estimate of the performance of the system, it needs to simulate a large number of transmitted bits. This operation has to be repeated for each MCS, each MIMO configuration, and each parameter to be studied. In order to simulate OFDM systems, we need to simulate N_{SD} (or more) subcarriers, the effect on noise on each of these subcarriers and their effect on the received blocks. Such a simulation can be very complex and time consuming.

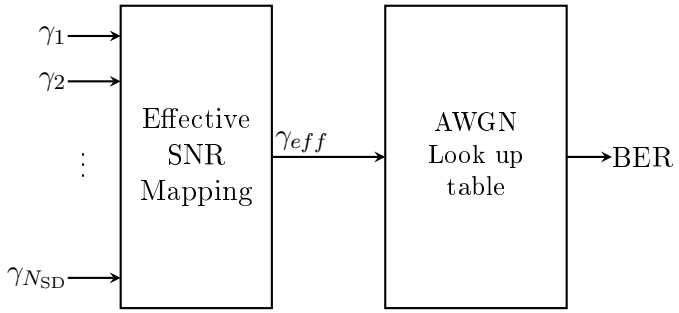

Figure 5.1: Functional block diagram for effective SNR mapping

These issues have motivated the widespread use of the Effective Exponential SNR Mapping (EESM) for OFDM based networks. For both cases, the exponential effective SNR mapping method simplifies the problem by mapping the vector of SNRs of each subcarrier into a single equivalent flat-fading SNR. EESM maps the SNRs of the N_{SD} subcarriers, $\gamma_1, \gamma_2, \ldots, \gamma_{N_{\mathrm{SD}}}$ into a single effective SNR value γ_{eff} as proposed from Ericsson [15]:

$$\gamma_{\mathrm{eff}} = -\beta \log \left(\frac{1}{N_{\mathrm{SD}}} \sum_{k=1}^{N_{\mathrm{SD}}} e^{-\frac{\gamma_i}{\beta}} \right) \tag{5.1}$$

where β is a parameter that is empirically calibrated according to the selected MCS The concept of effective SNR is mathematically expressed as follows

$$BER_{\mathrm{AWGN}}(\gamma_{eff}) \approx BER(\gamma_1, \gamma_2, \ldots, \gamma_{N_{\mathrm{SD}}}) \tag{5.2}$$

While there is no easy interpretation of the effective SNR mapping process, it should be observed that γ_{eff} is an exponential averaging of the SNR values experienced on each subcarriers, and as such, gives more weight to the low SNR values, corresponding to deep fades. Once β and the AWGN BER curve are known, the use of the EESM is very simple and is summarized in Figure 5.1.

5.2 Derivation of EESM

The EESM is derived based on the Union-Chernoff bound of error probabilities. The symbol error rate approximation for the constellations BPSK, QPSK, M-QAM over an

AWGN channel can be expressed as

$$\begin{aligned} P_e(d_{min}, \mathrm{SNR}) &\approx \bar{N}_{dmin} Q\left(\sqrt{\frac{d_{\min}^2}{2N_0}}\right) \\ &\overset{d_{\min}=2A}{=} \bar{N}_{dmin} Q\left(\sqrt{\frac{2A^2}{N_0}}\right) \\ &\overset{\mathrm{SNR}=KA^2/N_0}{=} \bar{N}_{dmin} Q\left(\sqrt{\frac{2\mathrm{SNR}}{K}}\right) \end{aligned} \tag{5.3}$$

where N_0 is the noise variance, $d_{min} = 2A$ is the minimum distance of constellation, $\bar{N}_{dmin}$ is the average number of nearest neighbors for the signal points in the constellation, and Q is the so called Q function

$$Q(x) = \frac{1}{\sqrt{2\pi}} \int_x^\infty e^{\frac{-t^2}{2}} \mathrm{d}t. \tag{5.4}$$

If the constellation scheme is Grey coded,the bit error probability can be approximated by the equation:

$$\begin{aligned} P_b(\mathrm{SNR}) &\approx \frac{1}{\log_2(M)} \bar{N}_{dmin} Q\left(\sqrt{\frac{2\mathrm{SNR}}{K}}\right) \\ &= aQ\left(\sqrt{\frac{\mathrm{SNR}}{b}}\right) \end{aligned} \tag{5.5}$$

Note that the parameters a, b are dependent on the constellation scheme. An upper bound of the Q function, is the Chernoff bound

$$Q(x) \leq e^{\frac{-x^2}{2}}, \quad x > 0. \tag{5.6}$$

Combining the Equations (5.5) and (5.6), the upper bound for the bit error probability is given by the equation

$$P_b(\mathrm{SNR}) \leq a e^{-\frac{\mathrm{SNR}}{2b}}. \tag{5.7}$$

Considering a SISO-OFDM system model with N_{SD} data subcarriers modulated by the same modulation coding scheme, and the SNR on each subcarrier being $\gamma_1, \ldots, \gamma_{N_{\mathrm{SD}}}$. We define the vector γ as follows

$$\gamma = \begin{bmatrix} \gamma_1 \\ \gamma_2 \\ \vdots \\ \gamma_{N_{\mathrm{SD}}} \end{bmatrix} \tag{5.8}$$

and considering that the MMSE or Zero Forcing detector output of each subcarrier corresponds to an equivalent Gaussian channel, the bit error probability for N_{SD} independent Gaussian channels is

$$\begin{aligned} BER(\gamma) &= \sum_{k=1}^{N_{\mathrm{SD}}} P_b(\gamma_k) \\ &\leq \sum_{k=1}^{N_{\mathrm{SD}}} a e^{-\frac{\gamma_k}{2b}}. \end{aligned} \tag{5.9}$$

The goal of EESM is to find an equivalent SNR value γ_{eff} which should be approximately equal to the SNR γ_{awgn} that would yield in an AWGN channel a BER equal to the actual instantaneous BER in a frequency-selective.

$$BER(\gamma_{\mathrm{eff}})\big|_{\gamma_{\mathrm{eff}} \approx \gamma_{\mathrm{awgn}}} \approx BER(\gamma) \tag{5.10}$$

So, taking mean of Equation (5.9) such that the single scalar γ_{eff} can map the set of N_{SD} SNRs as given below

$$\begin{aligned} & BER(\gamma_{\mathrm{eff}}) \approx \frac{1}{N_{\mathrm{SD}}} \sum_{k=1}^{N_{\mathrm{SD}}} a e^{-\frac{\gamma_k}{2b}} \Leftrightarrow \\ & a e^{-\frac{\gamma_{\mathrm{eff}}}{2b}} = \frac{1}{N_{\mathrm{SD}}} \sum_{k=1}^{N_{\mathrm{SD}}} a e^{-\frac{\gamma_k}{2b}} \Leftrightarrow \\ & -\frac{1}{2b}\gamma_{\mathrm{eff}} = \log\left(\frac{1}{N_{\mathrm{SD}}} \sum_{k=1}^{N_{\mathrm{SD}}} e^{-\frac{\gamma_k}{2b}}\right) \Leftrightarrow \\ & \gamma_{\mathrm{eff}} = -2b \log\left(\frac{1}{N_{\mathrm{SD}}} \sum_{k=1}^{N_{\mathrm{SD}}} e^{-\frac{\gamma_k}{2b}}\right) \Leftrightarrow \\ & \gamma_{\mathrm{eff}} = -\beta \log\left(\frac{1}{N_{\mathrm{SD}}} \sum_{k=1}^{N_{\mathrm{SD}}} e^{-\frac{\gamma_k}{\beta}}\right) \end{aligned} \tag{5.11}$$

where β is dependent on modulation coding scheme and has to be numerically optimized. As proposed in [16] the parameter β can be adjusted to match the EESM to a specific modulation scheme or, in the general case, a specific combination of modulation scheme and coding rate. The derivation of γ_{eff} starts with Chernoff upper bound which is not a tight bound for low SNR and other approximations are also used. So, a suitable β is not found to be equal to $2b$ after optimizing numerically. Thus, β is a correction factor which minimizes the mismatch between the actual BER and the estimated BER.

5.3 Calibration of EESM

The calibration of EESM is a process that must be done for everyone MCS separately. For each MCS shall be obtained the AWGN BER curve and the β parameter. Obtaining the AWGN BER curve for a given MCS requires performing a single link-level simulation. The Figure 5.2 shows the simulated system for the calculation of the AWGN BER curve. Fortunately, these are the simplest link level simulations since they do not require the modeling of a channel. This process is usually very fast and simple. To obtain the β value several channel realizations were created and for each channel realization, the BER can be obtained by simulations. The simulation results would then be compared with the reference BER curve obtained from AWGN channel under the same MCS level. There can be various optimization criteria to optimize β for each MCS. For example, two cost functions are presented in this section. The first one is

$$\beta_{\text{opt}} = \arg\min_{\beta}\left\{\frac{1}{N_C}\sum_{i=1}^{N_C}\Delta e_i(\beta)\right\} \tag{5.12}$$

where

$$\Delta e_i(\beta) = \frac{1}{L}\sum_{k=1}^{L}(\log_{10}(BER_{k,i}^{\text{meas}}) - \log_{10}(BER_{k,i}^{\text{EESM}}(\beta)))^2, \quad \forall i = 1, 2, \ldots, N_C \tag{5.13}$$

N_C is the number of different channel realizations considered for the optimization process, L is the number of different noise variances for each channel realization, $BER_{k,i}^{meas}$ is the measured BER for the i^{th} channel realization and k^{th}noise variance, and $BER_{k,i}^{EESM}(\beta)$ is the estimated BER for the given β, i^{th} channel realization and k^{th} noise variance. The second criterion is given by

$$\beta_{\text{opt}} = \arg\min_{\beta}\left\{\frac{1}{N_C}\sum_{i=1}^{N_C}(\gamma_{\text{AWGN}}(i) - \gamma_{\text{eff}}(i,\beta))^2\right\} \tag{5.14}$$

where $\gamma_{\text{eff}}(i,\beta)$ is the effective SNR computed with parameter β for the i^{th} channel realization, $\gamma_{\text{AWGN}}(i)$ is the required SNR to meet target BER under AWGN channel.

Once the AWGN BER curve and the optimal value of β are obtained, the EESM method can be used as often as needed. More specifically, for any channel matrix $\mathbf{H}$ and noise variance N_0 it can be estimated the BER value.

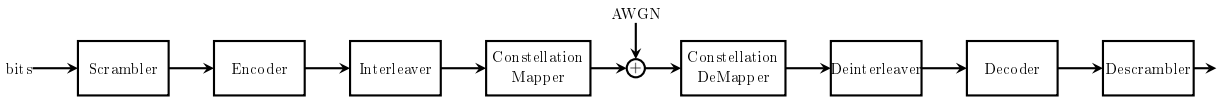

Figure 5.2: Block diagram of the used system to extract the AWGN BER curve.

5.4 Extension to Multiple Antenna Systems

So far we have discussed the implementation of the EESM method in a SISO-OFDM system. One of the big advantages of the EESM methodology is that it can be easily extended to cover multiple MIMO techniques. The basic idea of the method remains the same. The post-processing SNRs per subcarrier and spatial stream are mapped to one value, the effective SNR. When exists a single spatial stream the SNRs per subcarrier they can be computed by the equations which derived in the Chapter 4, and then the effective SNR is computed from the Equation (5.1).

Multiple Spatial Streams

The extension of EESM method in MIMO systems with multiple spatial streams is defined as [17]

$$\gamma_{\text{eff}} = -\beta \log \left(\frac{1}{N_{\text{SD}} N_{\text{SS}}} \sum_{j=1}^{N_{\text{SS}}} \sum_{k=1}^{N_{\text{SD}}} e^{-\frac{\gamma_{k,j}}{\beta}} \right) \tag{5.15}$$

It is well known that the Maximum Likelihood detector is non-linear and it may be necessary to use a simple linear approximation for the receiver to compute the per subcarrier SNR. In practice the ML detector doesn't used due to its high computational cost. If the ML detector is substituted by MMSE detector, the SNR definition in [18] for spatial streams under MIMO 2×2 can be expressed as $\gamma_{k,i}$ for i^{th} spatial stream and k^{th} subcarrier:

$$\gamma_{k,1} = \frac{\hat{N}_0 \cdot H_{k,1}^2 + |\det(\mathbf{H}_k)|^2}{\hat{N}_0(\hat{N}_0 + H_{k,2}^2)} \tag{5.16}$$

$$\gamma_{k,2} = \frac{\hat{N}_0 \cdot H_{k,2}^2 + |\det(\mathbf{H}_k)|^2}{\hat{N}_0(\hat{N}_0 + H_{k,1}^2)} \tag{5.17}$$

where

$$\mathbf{H}_k = \begin{bmatrix} h_{k,11} & h_{k,12} \\ h_{k,21} & h_{k,22} \end{bmatrix} \tag{5.18}$$

$H_{k,m}^2 = \sum_{i=1}^{2} |h_{k,im}|^2$,$\hat{N}_0$ is the noise variance after the FFT process, and $h_{k,ij}$ is complex channel parameter (in frequency domain) between i^{th} receiver and j^{th} transmitter for the k^{th} subcarrier., Further the post-processing per subcarrier and spatial stream SNRs when the Zero Forcing detector is used are:

$$\gamma_{k,1} = \frac{|\det(\mathbf{H}_k)|^2}{\hat{N}_0 H_{1,k}^2} \tag{5.19}$$

$$\gamma_{k,2} = \frac{|\det(\mathbf{H}_k)|^2}{\hat{N}_0 H_{2,k}^2} \tag{5.20}$$

Chapter 6

Simulation Environment & Performance Analysis

In this chapter we will present and analyze the simulation environment, and finally the numerical results. The simulator implements a HT OFDM system to simulate the 802.11n standard and is based on the Matlab WLAN Toolbox functions which implement basic components of the system on the transmitter and receiver. The simulations are made in two stages: in the first stage, end to end link level simulations are made over multiple channel realizations. Then, these results are used to tune the EESM parameter β.

6.1 System Environment & Assumptions

Five different systems are simulated, a SISO system system, a 1×2 SIMO system, a 2×1 MISO system by using Alamouti code and Transmit Beamforming, a 2×2 MIMO system with two spatial streams. The transmitter structure of all systems follows the standard 802.11n. In all systems a channel bandwidth 20MHz is used, binary convolutional encoder, and normal guard interval duration $T_{GI} = 800ns$. The PSDU length is determined for each MCS in order to the transmission duration of each packet remains the same. The structure of the receiver is shown in Figure 6.1, and the synchronization methods that used are explained in section 3.3.

At the simulation scenario the additive Gaussian noise signal impairments are added after the MRC or ZF detector as shown in Figure 6.1. The noise variances $\tilde{N}_0^{k,i}$ for each stream $\tilde{\mathbf{n}}_k^i$ per subcarrier and spatial stream are obtained subject to hold the following

equations

$$\gamma_k^i = \frac{f_1(\mathbf{H}_k^i)}{N_0}, \quad \forall\ 1 \le k \le N_{\mathrm{SD}}, 1 \le i \le N_{\mathrm{SS}} \tag{6.1}$$

$$\gamma_{aver} = f_2(\mathbf{H})\mathrm{SNR}_0 \tag{6.2}$$

$$\mathrm{SNR}_0 = \frac{f_0(\mathbf{H})}{N_0} \tag{6.3}$$

where the functions f_0, f_1, f_2 denotes the relations between SNR values as derived in Chapter 4. For example, in a SISO (a single spatial stream exists) system

$$\gamma_{aver} = \frac{N_{\mathrm{SD}}^2}{\sum_{k=1}^{N_{\mathrm{SD}}} \frac{1}{|h_k|^2} \sum_{k=1}^{N_{\mathrm{SD}}} |h_k|^2} \frac{N_{\mathrm{FFT}}}{N_{\mathrm{ST}}} \mathrm{SNR}_0 \Rightarrow f_2(H) = \frac{N_{\mathrm{SD}}^2}{\sum_{k=1}^{N_{\mathrm{SD}}} \frac{1}{|h_k|^2} \sum_{k=1}^{N_{\mathrm{SD}}} |h_k|^2} \frac{N_{\mathrm{FFT}}}{N_{\mathrm{ST}}} \tag{6.4}$$

$$\gamma_k = \frac{N_{\mathrm{FFT}}|h_k|^2}{N_{\mathrm{ST}} N_0} \Rightarrow f_1(h_k) = \frac{N_{\mathrm{FFT}}|h_k|^2}{N_{\mathrm{ST}}}, \tag{6.5}$$

$$\mathrm{SNR}_0 = \sum_{k=1}^{N_{\mathrm{ST}}} \frac{|h_k|^2|}{N_{\mathrm{ST}} N_0} \Rightarrow f_0(H) = \frac{|h_k|^2|}{N_{\mathrm{ST}}} \tag{6.6}$$

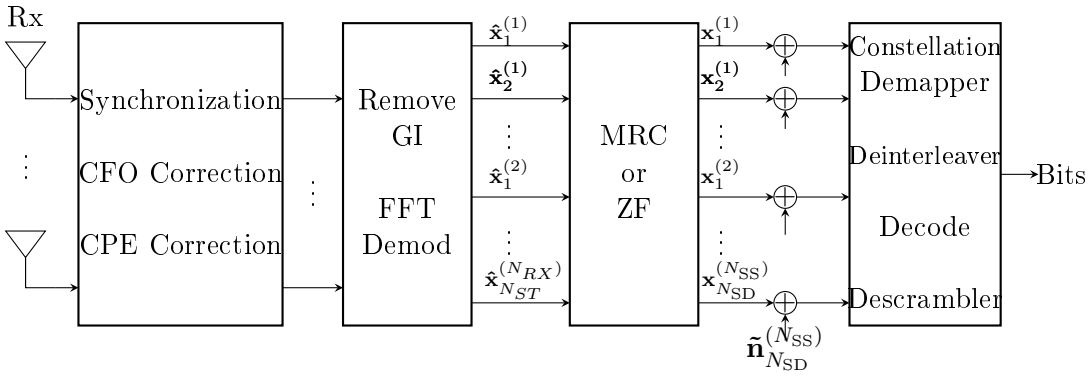

Figure 6.1: Block diagram of the receiver in simulations.

Since the FFT and MRC,ZF detectors are linear transformations, a simple method to compute the noise streams $\tilde{n}_k^i$ is presented in Figure 6.2. The steps of this method are the following

1. Calculation of the noise variance N_0 corresponding to the desired γ_{aver}.
2. Creation of AWGN noise signals $n^{(i)}(t) \sim \mathcal{CN}(0, N_0), i = 1, \ldots, N_{\mathrm{RX}}$ with duration equal to the duration of data portion of the packet.

3. Processing the noise signals from the FFT and linear detector modules.

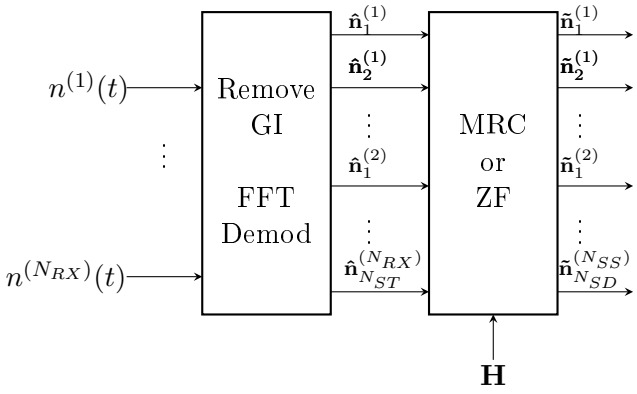

Figure 6.2: Block diagram of $\tilde{\mathbf{n}}_k^{(i)}$ calculation.

The extracted noise sequences are added to the equalized sequences of data $\mathbf{x}_k^{(i)}$ and the process of the receiver continues to the constellation demapper, deinterleaver, decoding, descrambler. As the synchronization and impairments correction methods applied to the noise free signal the following assumptions holds:

- Perfect packet synchronization and packet detection.
- Ideal carrier frequency offset estimation.
- Ideal channel estimation.
- Ideal common phase noise estimation.

Channel Description

To incorporate frequency selectivity, we have considered the IEEE channel models described in [19] mainly Model-B. The properties of this channel is provided in Table 6.1. Also we consider a transmitter-receiver distance of 10m. For Model-B when the distance between transmitter and receiver is greater than or equal to five meters, the model is NLOS. The Model-B simulates smaller environments as residential homes and small offices.

Table 6.1: IEEE Tgn Channel Model - B parameters.

Parameters	**Model - B**
Breakpoint distance (m)	5
RMS Delay (ns)	15
Maximum delay (ns)	80
Rician K-Factor (dB)	$0/-\infty$
Number of clusters	2
Number of taps	9

6.2 End to End Link Simulations

End to End link level simulations are performed over $N_C = 200$ channel realizations and L post - processing SNR values. For each channel realization and γ_{aver} combination, a transmission of $50 \cdot 10^6$ information bits are being simulated, which provides a good estimated bit error probability up to the order of 10^{-6}. Finally, each of the measured BER is obtained by averaging over the different noise realizations for a fixed MCS, channel realizations and post-processing SNR.

The results for the SISO system transmission through a time varying and static channel presented in Figure 6.3. In this simulations, the length in bits of the PPDU is adjusted to each MCS in order to the PPDU consists of 310 OFDM symbols.

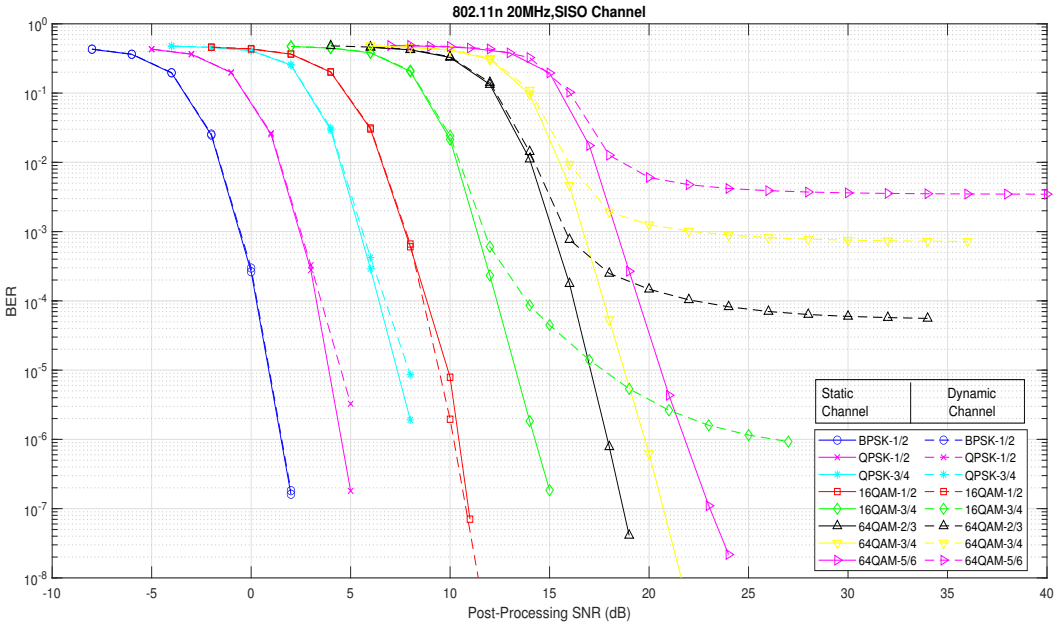

Figure 6.3: SISO HT OFDM system, BER vs γ_{aver} curve through dynamic and static channels.

The channel estimation for each packet, performed once a time by using the HT-LTF of the preamble. If the channel is varying over the time, the channel estimation accuracy decreases with the time. As a result if the channel is fast varying or the duration of the PPDU is long the performance of the system is low even if the noise variance tends to zero. We can observe that only the constellations 16 and 64 QAM are affected from the existing channel estimation error. This happens as the modulation order increases without being combined with increasing in transmit power, the system becomes more susceptible to channel estimation errors. Consequently its important to hold the length in bits of the PPDU fixed in order that in high order constellations the BER remains in low levels. To simplify the simulation environment, for the rest of the report we assume that the channel is static. The BER vs γ_{aver} curve for the SIMO 1×2 system is presented in Figure 6.3.

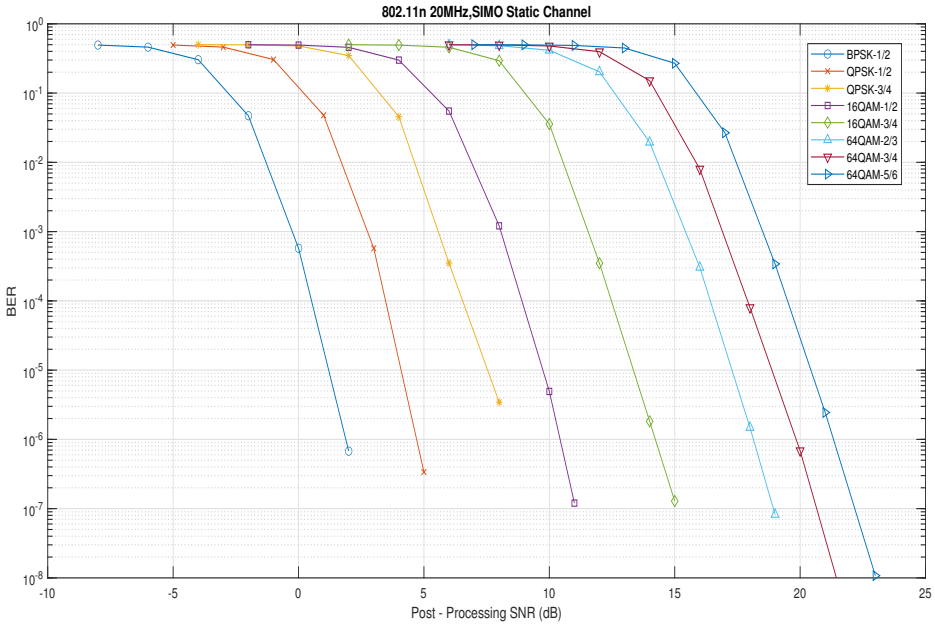

Figure 6.4: SIMO HT OFDM system, BER vs γ_{aver} curve through static channels.

The results for the MISO system 1×2 by using the Transmit Beamforming technique and the same channel realizations with the SIMO simulations, are identical to the SIMO curve. This is to be expected as well, from the analysis of the systems which done in Chapter 4.In addition the measured BER for the MISO system by using the Alamouti scheme, is equal to the SIMO if the noise variance decreased to the half. Therefore the BER vs γ_{aver} curves are shifted by 3dB at left.

Finally, we present in Figure 6.5 the results for the MIMO 2×2 system, with two spatial streams.

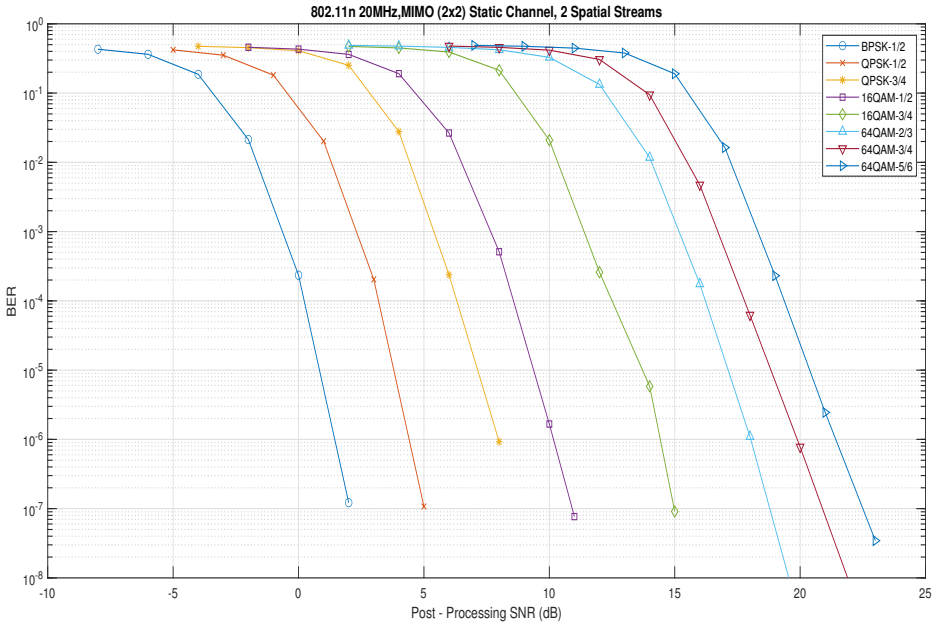

Figure 6.5: MIMO HT OFDM system, BER vs γ_{aver} curves through static channels.

6.3 EESM Tuning

In this section we will explain how the EESM method is tuned over all the MCS and MIMO systems. As we explain in section 5.3, the usage of the EESM is based on the AWGN BER curve, and the β parameter which is dependent on the MCS and it shall be optimized. The AGWN BER curve is obtained by a link simulation. To decrease the complexity of the AWGN system, the OFDM modulation can be ignored and the system is simplified as is shown in Figure 5.2. The full simulated $N_C = 200$ channel realizations of the previous section would used to tune and validate the β parameter. The first 100 channel realizations over all the SNR points are used to obtain the optimal value of β parameter, and the last 100 channel realizations are used to evaluate the EESM performance. The optimal β value selected to be that which minimizes the Mean Square Error in the $\log_{10}$(BER) domain,

$$\beta_{\text{opt}} = \arg\min_{\beta} \text{MSE}(\beta) = \left\{ \frac{1}{N_{\text{points}}} \sum_{i=1}^{N_{\text{points}}} \Delta e_i(\beta) \right\} \tag{6.7}$$

where

$$\Delta e_i(\beta) = (\log_{10}(BER^i_{\text{EESM}}(\beta)) - \log_{10}(BER^i_{\text{meas}}))^2, \tag{6.8}$$

N_{points} is the total number of different pairs channel realization / noise variance, BER^{i}_{meas} is the measured BER for the i^{th} channel realization and noise variance, and $BER^{i}_{\text{EESM}}(\beta)$ is the estimated BER for the given β, and i^{th} channel realization noise variance. Since the β_{opt} tends to be close to 1 for BPSK and QPSK, and tends to increase when the modulation order or the coding rate is increasing, the optimal value β can be obtained by using exhaustive search subject to the domain of the problem, e.g for the BPSK modulation, the domain can be defined as the vector $[0.5 : 0.01 : 2]$. In the Figure 6.6 presented the MSE vs β graph subject to the domain $\beta \in [7 : 0.01 : 14]$.

Input: **b** : Vector which contains the β values (domain of the problem) e.g
b $= [0.5 : 0.01 : 2]$
Input: $\gamma^{j}_{k,i}$,$BER^{i}_{\text{meas}}, i = 1, \ldots, N_{\text{points}}, k = 1, \ldots, N_{\text{SD}}, j = 1, \ldots, N_{\text{SS}}$
Output: MSE,β_{opt}
Obtain the AWGN BER vs SNR curve;
m = 0;
for $\beta \in$ **b do**
  m = m + 1;
  for $i = 1 : N_{\text{points}}$ **do**
    Compute γ_{eff} by using the β value and the per subcarrier SNRs $\gamma^{j}_{k,i}$ from the Equation 5.15 ;
    $BER^{i}_{\text{EESM}} = BER_{\text{AWGN}}(\gamma_{\text{eff}})$;
  end
  Compute the MSE(m) value by using the Equation 6.7;
end
Find the index idx that corresponds to the minimum value of MSE vector;
return **b**(idx), MSE(idx);

Algorithm 1: Parameter β calibration algorithm.

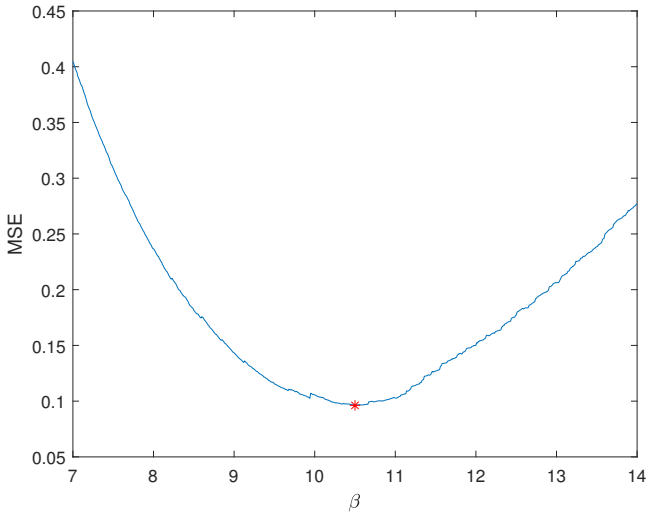

Figure 6.6: Cost function graph versus the β parameter for a SISO system, QPSK modulation and coding rate $R = 3/4$.

SISO System

Let us denote with $MSE_{\text{opt}}(\beta)$ the mean square error which produced from the first 100 channel realization and with $MSE_{\text{valid}}(\beta)$ the mean square error which produced from the last 100 channel realizations. The optimal β values are tabulated in Table 6.2. In addition is presented the two mean square values for each MCS. In theory, the parameter $\beta = \beta_{\text{opt}}$ value would be optimal if its minimizing the mean square error over the infinite(or a large number) of channel realizations which can be occur. However, a small number of channel realizations is used to obtain the β parameter due to the high computational time of full link simulations. The difference $MSE_{\text{opt}}(\beta_{\text{opt}}) - MSE_{\text{valid}}(\beta_{\text{opt}})$ is an indicator of if the sub optimal β value is tends to be optimal.

Table 6.2: EESM optimal β parameter for SISO 20MHz system.

MCS	β_{opt}	$\textbf{MSE}_{\text{opt}}(\beta_{\text{opt}})$	$\textbf{MSE}_{\text{valid}}(\beta_{\text{opt}})$
0	1.22	0.0368	0.0422
1	2.35	0.0508	0.0715
2	2.23	0.0711	0.0750
3	8.58	0.0686	0.0643
4	10.50	0.0962	0.0822
5	40.19	0.1402	0.1295
6	41.85	0.0943	0.0884
7	41.25	0.0812	0.0835

The Figure 6.7 will help us to understand the next graphs that will be presented. The solid line corresponds to the AWGN BER vs SNR curve for the MCS 2 of the SISO 20MHz channel. The points which are scattered around the curve, are the measured BER for a channel realization and 7 noise variances. The coordinates of these points are $(\gamma_{\text{eff}}, BER_{\text{meas}})$. Thus, the estimate of BER for one channel realization and noise variance by means of EESM, is the point where the vertical line as shown in the figure, it intersects the AWGN graph.

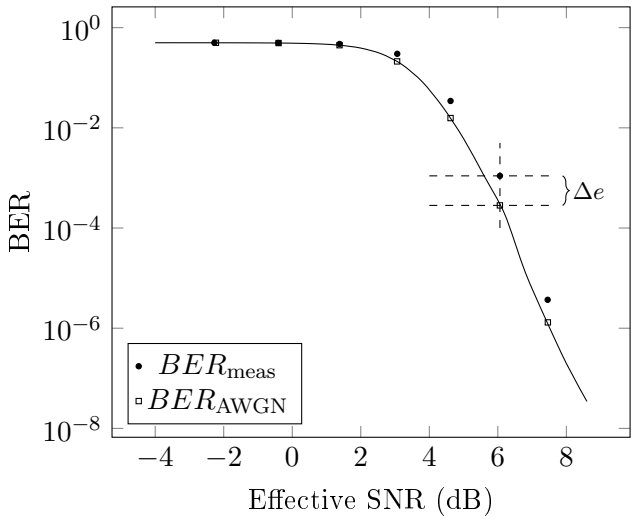

Figure 6.7: BER estimates by means of EESM, and measured probabilities respectively, for 20MHz SISO channel, and MCS 2.

In Figure 6.8 shown the measured BERs values, and the AWGN curve for each MCS 0 to 7. We can observe that for higher modulation orders and / or coding rates the estimated error increases. However, the mean estimated BER for a specific post-processing SNR value strictly approximates the average measured BER as we can observe in Figure 6.9

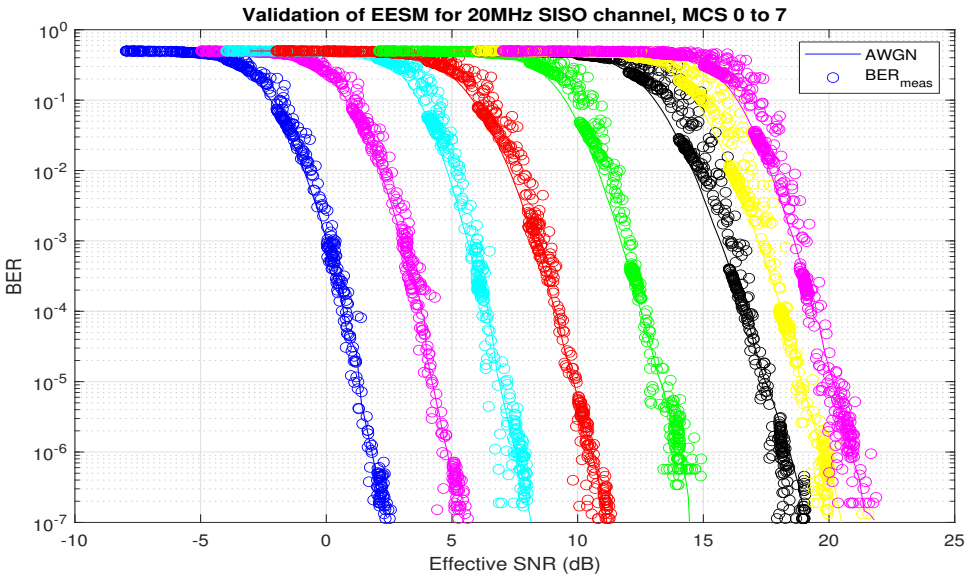

Figure 6.8: EESM validation for SISO channel.

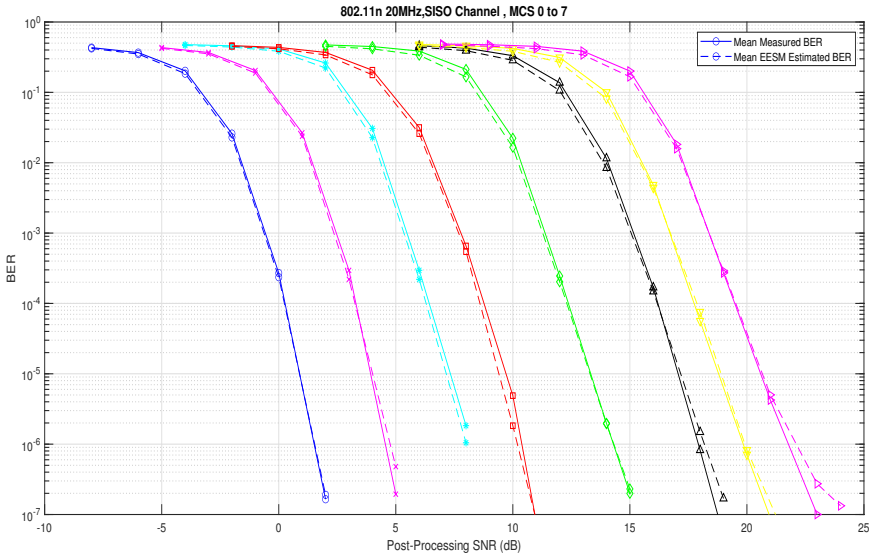

Figure 6.9: Average measure and estimated BER over 200 channels realizations.

SIMO System

For the 20MHz SIMO channel system, the numerical results presented in Table 6.3. Note that for a MISO system which using the Transmit Beamforming technique, the β values is equal to the SIMO. On the other hand, for a MISO system which uses an Alamouti scheme the per subcarrier SNR is decreased in half, and optimal β values differ.

Table 6.3: EESM optimal β parameter for SIMO 20MHz system.

MCS	β_{opt}	$\mathbf{MSE}_{\text{opt}}(\beta_{\text{opt}})$	$\mathbf{MSE}_{\text{valid}}(\beta_{\text{opt}})$
0	1.07	0.0399	0.0345
1	2.22	0.0426	0.0422
2	2.00	0.0226	0.0215
3	8.02	0.0210	0.0350
4	9.47	0.0237	0.0255
5	40.19	0.0387	0.0410
6	41.54	0.0199	0.0243
7	39.24	0.0185	0.0183

Assessing the results from the Figure 6.10 and the Table 6.3, we conclude that the 100 random channel realizations sufficient for a good estimate of the optimal value of β.

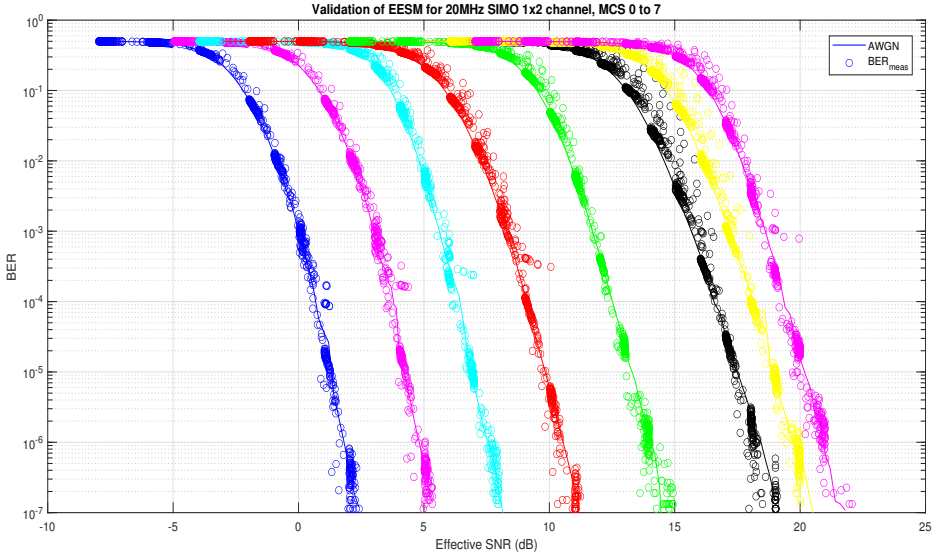

Figure 6.10: EESM validation for SIMO 1×2 channel.

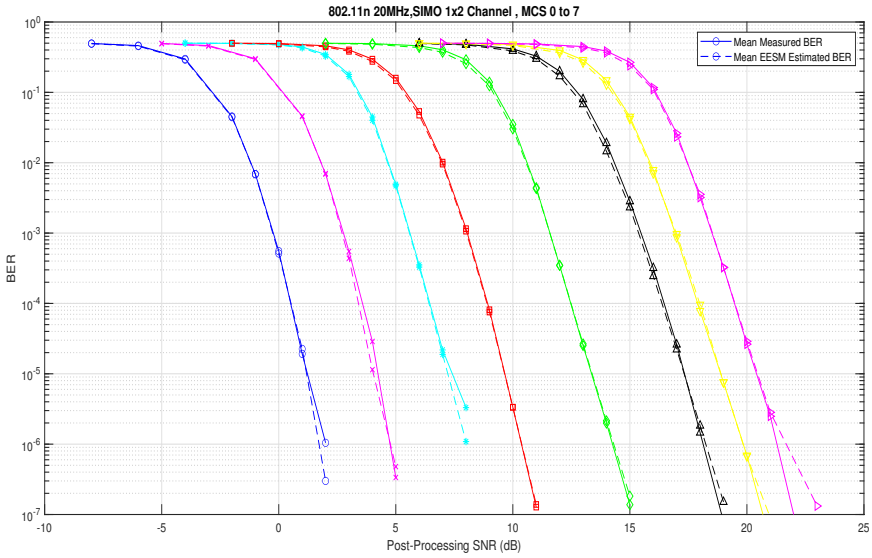

Figure 6.11: Average measure and estimated BER over 200 channels realizations for 20MHZ SIMO 1×2 Model-B channel.

MIMO system

Since in the MIMO system 2×2 , two spatial streams are exists, the number of different SNRs which are used in the computation of effective SNR γ_{eff}, is doubled. Studying the Tables with the numerical results about MSEs, it is obvious that for higher MCS rates, EESM performance decreases. This may be due to the interference which is not taken into account in our project.

Table 6.4: EESM optimal β parameter for MIMO 20MHz system.

MCS	β_{opt}	$\mathbf{MSE}_{\text{opt}}(\beta_{\text{opt}})$	$\mathbf{MSE}_{\text{valid}}(\beta_{\text{opt}})$
8	1.22	0.0766	0.0527
9	2.52	0.1165	0.0848
10	2.36	0.1035	0.1151
11	8.98	0.0656	0.0640
12	10.71	0.1691	0.1352
13	35.12	0.1000	0.1004
14	40.74	0.0977	0.1014
15	43.76	0.1272	0.1040

In Figure 6.12 we observe that there is an increased estimation error in the value range $[3 \cdot 10^{-1}\ 10^{-2}]$ where the curve shows increased curvature and the BER starts to decrease drastically. This is due to parameter β which is not able to minimize the error in all slopes of the curve. Finally in Figure 6.13 is observed that the tight correspondence between the actual average BER and the estimated, is holds and in MIMO channels

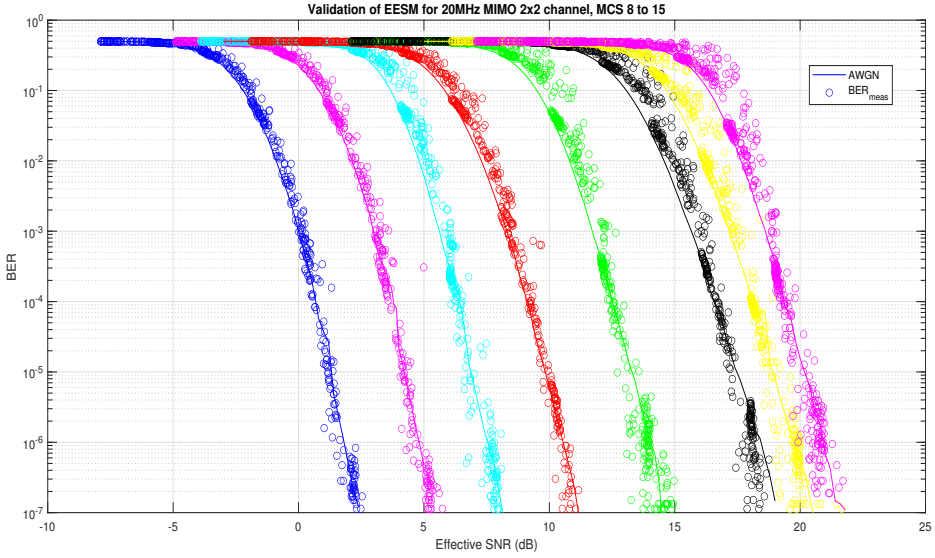

Figure 6.12: EESM validation for MIMO channel.

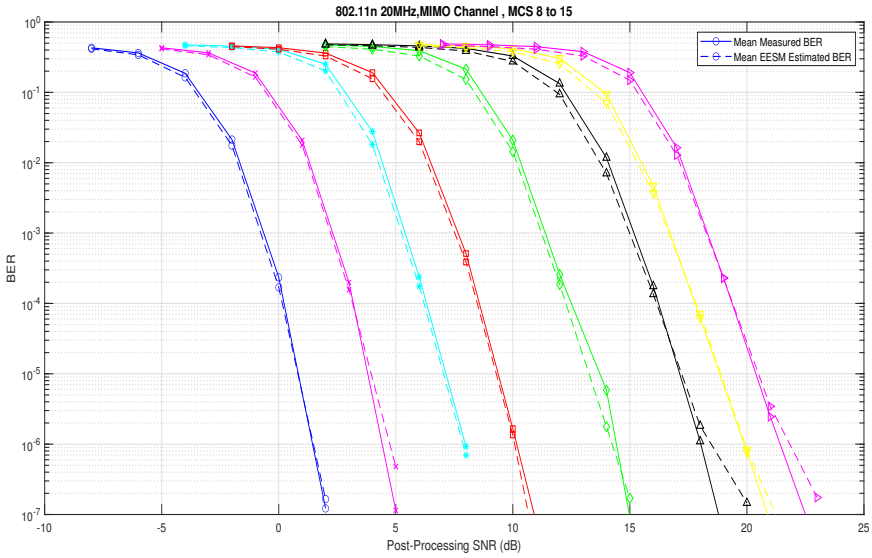

Figure 6.13: Average measure and estimated BER over 200 channels realizations for 20MHZ MIMO Model-B channel.

Chapter 7

Conclusion

The IEEE 802.11n(High Throughput format) was proposed in 2009 and is the first standard which supports MIMO channels up to 4×4, larger channel bandwidth and adaptive modulation coding technique in order to increase throughput. The standard 802.11n is based on the HT PPDU format and used OFDM transmissions. The amendments 802.11ac(Very High Throughput format), 802.11ax (High Efficiency format) is based on the 802.11n standard, extends further the bandwidth, increases the maximum modulation order and the number of antennas to achieve higher data rates where they are required nowadays by society. Different variants of the OFDM method are widely used in the latest and next generation WLANs. The continuous increase of the complexity of the systems, has become time consuming the evaluation of the systems by using full link level simulations. In addition the adaptive modulation coding technique requires a fast prediction of the BER / PER and the instantaneous channel state. The realm of this project is to study the EESM method and provide efficient link level simulations with low complexity cost for the 802.11n standard. EESM is suitable for OFDM systems, as it maps the SNRs per subcarrier to one scalar value which used to estimate the total of system performance.

The basic fundamentals of the OFDM and MIMO decoding techniques were introduced. OFDM achieves high spectral efficiency by overlapping the frequency response of the subchannels. The subcarriers are orthogonal and OFDM decouples the frequency selective fading channel into parallel flat fading channels. MIMO provides array and diversity gains. The details of the 802.11n PPDU format, the transmitted signal, and the structure of the HT OFDM system are presented. Three SNR values at different stages of the receiver are defined. Furthermore, the background theory of the EESM method was introduced.

The system as simulated by using the Matlab WLAN Toolbox. Ideal packet detection, CFO, CPE, and channel estimation is assumed. End-to-end simulations were done through random channel realizations of IEEE channel mode-B, exported the average BER vs post-processing SNR curve per MCS. Further, the optimal β parameter of EESM and the AWGN BER curves per MCS are obtained. Finally, the BER vs post-processing SNR per MCS

curves, are estimated by using the EESM method.

The BER vs SNR mapping results for frequency selective channels shows close concurrence with AWGN results which makes EESM acceptable for abstraction in system level simulation to improve time efficiency. Furthermore, the estimated average BER vs SNR over a large number of random channel realizations is a good approximation of the actual mean BER curve. Since the basic advantage of EESM is that it is calibrated once, and after that can be used as often as needed, the EESM method can be used to estimate the performance of the system for each parameter to be studied with a very low complexity. Further, it can be employed as a link adaptation algorithm.

Future works in this topic may focus on investigating of the EESM performance by handling the interference cases using the signal to Interference plus noise ratio instead of the signal to noise ratio. In addition, the EESM method can be evaluated in larger bandwidths, and higher Modulation schemes as 1024-QAM which provided from 802.11ax standard.

Bibliography

[1] Gagandeep Singh, Shelza, and Sukhvir Singh. "IEEE 802.11 WLAN and Advancements: A Review". In: 2014.

[2] A. Peled and A. Ruiz. "Frequency domain data transmission using reduced computational complexity algorithms". In: *ICASSP '80. IEEE International Conference on Acoustics, Speech, and Signal Processing*. Vol. 5. 1980, pp. 964–967. DOI: 10.1109/ICASSP.1980.1171076.

[3] https://www.tdx.cat/bitstream/handle/10803/6886/04Hidw04de10.pdf?jsessionid=D7DCE01D. Accessed: 2021-09-20.

[4] Proakis. *Digital Communications 5th Edition*. McGraw Hill, 2007.

[5] Georgia Ntogari, Thomas Kamalakis, and Thomas Sphicopoulos. "Performance Analysis of Space Time Block Coding Techniques for Indoor Optical Wireless Systems". In: *IEEE Journal on Selected Areas in Communications* 27.9 (2009), pp. 1545–1552. DOI: 10.1109/JSAC.2009.091204.

[6] "IEEE Standard for Information technology–Telecommunications and information exchange between systems Local and metropolitan area networks–Specific requirements Part 11: Wireless LAN Medium Access Control (MAC) and Physical Layer (PHY) Specifications". In: *IEEE Std 802.11-2012 (Revision of IEEE Std 802.11-2007)* (2012), pp. 1–2793. DOI: 10.1109/IEEESTD.2012.6178212.

[7] T.M. Schmidl and D.C. Cox. "Low-overhead, low-complexity [burst] synchronization for OFDM". In: *Proceedings of ICC/SUPERCOMM '96 - International Conference on Communications*. Vol. 3. 1996, 1301–1306 vol.3. DOI: 10.1109/ICC.1996.533620.

[8] Tzi-Dar Chiueh and Pei-Yun Tsai. *OFDM Baseband Receiver Design for Wireless Communications*. Wiley Publishing, 2007. ISBN: 0470822341.

[9] P.H. Moose. "A technique for orthogonal frequency division multiplexing frequency offset correction". In: *IEEE Transactions on Communications* 42.10 (1994), pp. 2908–2914. DOI: 10.1109/26.328961.

[10] A. van Zelst and T.C.W. Schenk. "Implementation of a MIMO OFDM-based wireless LAN system". In: *IEEE Transactions on Signal Processing* 52.2 (2004), pp. 483–494. DOI: 10.1109/TSP.2003.820989.

[11] D.P. Bertsekas and J.N. Tsitsiklis. *Introduction to Probability*. Athena Scientific books. Athena Scientific, 2002. ISBN: 9781886529403.

[12] Ingmar Land, Peter A. Hoeher, and Snjezana Gligorevic. "Computation of symbol-wise mutual information in transmission systems with LogAPP decoders and application to EXIT charts". English. In: *Proceedings of the International ITG Conference on Source and Channel Coding, Erlangen*. ©2004 IEEE. Personal use of this publication is permitted. However, permission to reprint/republish this material for advertising or promotional purposes or for creating new collective works for resale or redistribution to servers or lists, or to reuse any copyrighted component of this work in other works must be obtained from the IEEE. ISSN ? -? Computation of symbol-wise mutual information in transmission systems with LogAPP decoders and application to EXIT charts ? Conference date: 19-05-2010. Germany, 2004, pp. 195–202.

[13] A.J. Viterbi. "An intuitive justification and a simplified implementation of the MAP decoder for convolutional codes". In: *IEEE Journal on Selected Areas in Communications* 16.2 (1998), pp. 260–264. DOI: 10.1109/49.661114.

[14] Sébastien Simoens et al. "Error prediction for adaptive modulation and coding in multiple-antenna OFDM systems". In: *Signal Processing* 86.8 (2006). Special Section: Advances in Signal Processing-assisted Cross-layer Designs, pp. 1911–1919. ISSN: 0165-1684. DOI: https://doi.org/10.1016/j.sigpro.2005.09.033. URL: https://www.sciencedirect.com/science/article/pii/S0165168405003956.

[15] Ericsson. "System-level evaluation of OFDM – further considerations". In: 2003.

[16] M. Pauli U. Wachsmann and S. Tsai. *Quality determination for a wireless communications link*. Tech. rep. Patent US 2004/0219883, 2004.

[17] Thomas R. Hendersons Rohan Patidar Sumit Roy. *Technical report on validation of error models for 802.11n*. Tech. rep. University of Washington Seattle, Department of Electrical Engineering, 2017.

[18] Hao Liu et al. "EESM Based Link Error Prediction for Adaptive MIMO-OFDM System". In: *2007 IEEE 65th Vehicular Technology Conference - VTC2007-Spring*. 2007, pp. 559–563. DOI: 10.1109/VETECS.2007.126.

[19] P. Kyritsi Vinko Erceg V. L. Schumacher. "IEEE P802.11 Wireless LANs TGn Channel Models". In: 2004.